Sodium Chlorate Oxygen Generation for Fuel Cell Power Systems

by

Jorge David Garcia

B.S., Mechanical Engineering
United States Naval Academy, 2015

Submitted to the Department of Mechanical Engineering
in Partial Fulfillment of the Requirements for the Degree of

Master of Science in Mechanical Engineering
at the
Massachusetts Institute of Technology

June 2017

Signature redacted

Signature of Author: _____
Department of Mechanical Engineering
May 12, 2017

Signature redacted

Certified by: _____
Douglas P. Hart
Professor of Mechanical Engineering
Thesis Supervisor

Signature redacted

Accepted by: _____
Rohan Abeyaratne
Professor of Mechanical Engineering
Chairman, Committee for Graduate Students

Sodium Chlorate Oxygen Generation for Fuel Cell Power Systems

by

Jorge David Garcia

Submitted to the Department of Mechanical Engineering on May 12, 2017
in Partial Fulfillment of the Requirements for the Degree of
Master of Science in Mechanical Engineering

Abstract

In this thesis we experimentally investigated the use of sodium chlorate as an oxygen storage medium for use in underwater fuel cell power systems. Research into improving hydrogen storage systems is the primary concern when designing fuel cell systems with access to atmospheric oxygen. However, in an underwater environment, performance of the oxygen storage system cannot be overlooked. Oxygen candles using sodium chlorate offer gravimetric storage densities similar to compressed gas storage while also offering volumetric storage densities greater than both gas and cryogenic liquid oxygen storage. Unfortunately, this technology does not allow for controllable rates of oxygen production and is known to cause fires and occasionally explosions when contaminated with organic materials or exposed to external sources of heat. Though useful as an emergency source of oxygen, sodium chlorate will not be viable for use in power systems until safer and more controllable methods of releasing its oxygen are implemented.

During this project we developed a batch method for releasing oxygen from sodium chlorate. Two grams of sodium chlorate with nanoscale cobalt oxide catalyst were loaded into a reaction chamber and heated until decomposition. Afterwards a piston was used to eject the materials from the reaction chamber. This method proved to be safer and more reliable than similar chlorate-based oxygen systems as the primary modes of failure, those associated with the buildup of solid residue at the inlets and exits of the reaction chamber, were removed. Aside from preventing the flow of oxygen to a fuel cell, the over-pressurization caused by these problems could compromise the reaction chamber and potentially result in catastrophic failures. The achieved rate of oxygen production, 0.21 L/min with a heating rate between 25 W and 33 W, was below the target 1.13 L/min needed to operate a 200 W PEM fuel cell. Further assessment of this method will require the use of a more active cobalt oxide catalyst, a system with a larger reaction chamber capable of decomposing increased amounts sodium chlorate per cycle and a reduction in heat losses through the use of improved insulation and thermal isolation techniques.

Thesis Supervisor: Douglas P. Hart
Title: Professor of Mechanical Engineering

Acknowledgments

Thank you to all my friends and family for keeping me sane and helping me get to where I am today! Your love, patience and mentorship over the years has been essential in my growth as a (semi-)reasonable human being, an engineer and a naval officer.

To mom, dad, Sonia and Max, I miss you and regularly get homesick. I look forward to every visit and cherish the time we spend together. I want to properly represent our family and make you proud.

To Bito, Mike and Adam, you guys are like family and drop what you are doing every time I go home. Your continued friendship over the years has proven to be invaluable.

To my advisor Doug, John V. over at Beaverworks, Nick Pulsone at Lincoln, Mark Belanger at Edgerton and all the members of Doug's Fun House, thank you for the engineering and life guidance, the teaching moments and the general lab awesomeness. I've learned a lot while at MIT and couldn't have hoped for a better environment and group of people to work with. To Doug, that shifty Army kid can't be trusted. Keep an eye on him and don't let him near your boat. To Kelsey, Canada is overrated. To Mark, keep improving upon your ping pong skills. Eventually we'll have a competitive match. To the West Point kid in our lab, *Go Navy, Beat Army!*

To my roommates, Craig, Ben and Quan, and my mexican food loving friend PK, thanks for the good times, for putting up with my nonsense and for getting me to leave the apartment once in a while. I will miss you guys and all the tennis, ping pong and random debates we engaged in.

This work was supported by the Office of Naval Research under program manager Dr. Mike Wardlaw, and by Lincoln Laboratory with guidance from Dr. Nicholas Pulsone of the Advanced Undersea Systems and Technology group.

THIS PAGE INTENTIONALLY LEFT BLANK

Contents

1 Introduction **15**
- 1.1 Motivation . . . 15
- 1.2 Approach . . . 17
- 1.3 Organization . . . 18

2 Background **21**
- 2.1 Power Systems for Underwater Vehicles . . . 21
- 2.2 Oxygen Systems and Storage . . . 24
- 2.3 Chlorate-based Oxygen Storage . . . 30
- 2.4 Chemistry . . . 38
- 2.5 Hydrogen Storage Selection . . . 42

3 Materials and Methods **47**
- 3.1 Equipment and Software . . . 47
- 3.2 Chemicals . . . 48
- 3.3 Storage and Safety . . . 48

4 Thermal Analysis and Mixture Preparation **49**
- 4.1 Thermal Analysis of $NaClO_3$ . . . 49
- 4.2 Disagreement with literature results . . . 60

5 Prototype Development **67**
- 5.1 Bead Chain System . . . 68
- 5.2 Batch Piston System . . . 73

6 Summary and Conclusions **81**

Appendices **83**

A Hydrogen and Oxygen Storage Selection **85**
- A.1 Reactant Storage Metrics . . . 85
- A.2 Reactant Storage ED and SE Calculations . . . 87

B Oxidant and Catalyst Properties **91**

C Additional SEM Images **93**

THIS PAGE INTENTIONALLY LEFT BLANK

List of Figures

1-1 Breaking a complex problem down into independent steps allows for the most critical areas to be identified and ultimately addressed. . . . 18

2-1 The U-212 fuel cell power system, which can generate up to 450 kW, uses cryogenic oxygen storage and metal hydride hydrogen storage, both located outside of the pressure vessel [4, 5]. 23

2-2 The Urashima's fuel cell power system is rated at 4 kW. Its hydrogen is stored in a metal hydride system [10]. 24

2-3 The schematic shows that cryogenic storage systems can be rather complicated, requiring support architecture such as pre-heaters, humidifiers and radiators [14]. 26

2-4 Cryogenic storage systems are a proven technology with energy densities greater than secondary silver-zinc and lithium batteries. Advertised as having a $200 refueling cost, Sierra Lobo's power system is more economical than primary lithium ion batteries which, despite similar energy densities, can cost as much as $100,000 per use [14]. . . 26

2-5 This system used 80% concentrated hydrogen peroxide solution. Additional water was added to the combustion chamber to limit the temperature of the reaction and provide more steam to pass through the turbine [15]. 27

2-6 Oxygen candles are only used once, typically during emergency situations, and are designed to be self-sustaining. The insulation and housing help maintain the high internal temperatures needed for complete combustion while also preventing damage to surrounding equipment. 31

2-7 In order to prevent lithium perchlorate from prematurely melting and causing the system to fail, the engineers added heat shielding to the powder distributor. One advantage of using lithium perchlorate instead of sodium chlorate is that the lithium chloride byproduct melts at 605°C, well below the 800°C required to melt sodium chloride, making it easier to transport. 32

2-8 Storing lithium perchlorate as a liquid simplifies transport into the reaction chamber; however, premature decomposition around the injection port can result in system failure. Lithium chloride waste has a higher melting point than lithium perchlorate, meaning it will form as a solid and eventually plug the port. 33

2-9 Decomposing aqueous lithium chlorate first requires that the water be evaporated. A water rinse is also used to remove the solid lithium chloride waste from the reaction chamber. As these processes significantly increase this system's energy requirements, the engineers at API designed an integrated system that utilizes fuel cell waste heat [26]. . 35
2-10 Returning the waste products to the reactant storage container would improve this system's volumetric and gravimetric oxygen storage densities by eliminating the space and weight occupied by a separate waste container [27]. 36
2-11 This reactor was designed to store some of the released oxygen gas, decreasing the risk from over-pressurization and allowing for variable oxygen demand [27]. 37
2-12 Most of the components in this system were made from stainless steel. The authors recommended future systems utilize lighter oxygen compatible materials, thereby increasing the system's gravimetric storage density [27]. 37
2-13 Thermogravimetric analysis showed that approximately 50% of the available oxygen had decomposed at 475°C. This was accompanied by exothermic behavior between 460°C and 530°C, observed during differential thermal analysis [17]. 39
2-14 The authors heated 9.8 mg of sodium chlorate at 10°C/min. Results showed onset and final decomposition temperatures of 521°C and 583°C, respectively [2]. 41
2-15 The results showed that nanoscale cobalt oxide catalyst can result in significant decomposition while sodium chlorate is still in the solid phase [2]. 41
2-16 Ideal power systems offer high volumetric and gravimetric energy densities, while maintaining average densities near that of seawater. Underwater vehicles can deviate somewhat from neutral buoyancy through the use of drag-inducing lifting surfaces. 45

4-1 Decomposing near its melting point significantly reduces heating requirements for the 3% by weight nanoparticle cobalt oxide mixture. . 51
4-2 Results confirmed that decreased catalyst particle sizes and increased catalyst weight percentages resulted in lower decomposition temperatures. 52
4-3 Significant portions of the samples decomposed before elevated temperatures were achieved, thus preventing potentially higher rates of decomposition from being observed. 54
4-4 These results showed that, for a sodium chlorate mixture containing 6.7% by weight nanoscale cobalt oxide, 350°C is a suitable operating temperature. 55
4-5 Though not performed, it is suspected that using temperature ramp rates greater than 100°C/min would have resulted in the observation of even faster rates of decomposition. 56

4-6 Though useful as a chlorine suppressant, lithium peroxide does not substantially reduce sodium chlorate's decomposition temperatures. . 57
4-7 The inclusion of only small amounts of lithium peroxide suppresses the catalytic effect of cobalt oxide. Increased amounts of lithium peroxide seemed to have no additional effects. 59
4-8 Agglomeration of the catalyst could explain the different surface areas advertised by the supplier and measured by this author. The agglomerates acted as larger particles with smaller specific surface areas would. 62
4-9 Samples A and B, containing 3% by weight cobalt oxide, were found in the literature, while samples C and D, containing 6.7% cobalt oxide, were prepared by this author. Samples B and C were prepared using similar procedures. 64
4-10 Different TGA testing procedures and sample mixing techniques played only a minor role in the discrepancy between these results and those in the literature. The differences were likely due to inadequate preparation/storage of the nanoscale catalyst, either by this author or the supplier. 65

5-1 The samples were contained in a 316 stainless steel beaker and the hot plate was maintained at approximately 500°C. Transitioning from being a solid to a liquid and finally back to being a solid complicates the transport of sodium chlorate mixtures into and out of a reaction chamber. The exothermic release of heat during decomposition also has the potential to prematurely melt portions of the mixture or possibly damage the system due to spikes in temperature. 68
5-2 The tubing and hopper assembly was supported with a typical laboratory stand. The ball chain was threaded through the tubing and connected end-to-end. 69
5-3 As with the previous experiment, this assembly was mounted in the fume hood with a laboratory stand. 70
5-4 Experimental schematic of the final bead chain prototype. 71
5-5 Though simple in design, this system struggled to transport the fully liquid material and was prone to jamming. Utilizing a more active cobalt oxide catalyst may improve results, as some of the mixture would decompose prior to reaching the melting point and thus not enter a liquid state. 71
5-6 The 304 stainless steel chain suffered from corrosion during longer tests. Sodium chlorate melt also tended to fill the hollow beads during transport through the reaction chamber, reducing flexibility of the chain. . 72
5-7 Despite the open construction of the reaction chamber, it was expected that only a small percentage of sodium chlorate would leak from the system. Due to its high melting point, any sodium chlorate leaking from the reaction chamber quickly freezes, preventing further loss of material. 73

5-8 To avoid material corrosion issues, the piston and tubing were made from 316 stainless steel. This proved effective, as undesired species were not observed in the waste materials. 74
5-9 The discoloration of the stainless steel was due to high temperature growth of the oxidation layer and not chemical corrosion. The brown and purple colors on the outside of the tube, observed during this test and others, suggest that local temperatures were between 390°C least 450°C [40]. 76
5-10 Using a piston to physically sweep the reaction chamber meant that failures due to the gradual buildup of frozen reactants and waste materials, the most common failure mode for these types of systems, is unlikely to occur. 77
5-11 Further refinement and more careful design of this batch process is needed. During one test, the piston head rested lower inside the reaction chamber than was intended. This reduced the temperature of the piston head and the adjacent reactants, resulting in incomplete decomposition (right). 77

List of Tables

2.1 The Urashima typically operates autonomously and has a hybrid power system allowing for considerable cruising distances [10]. 24

2.2 Sodium chlorate stores nearly as much oxygen as LOX but, when used in formulations without metal fuels, is inherently safer [11, 18]. 29

2.3 LOX has the best gravimetric oxygen storage capacity, due to it being a pure substance, but the chemical storage methods can provide better volumetric oxygen storage. Note that this comparison does not include the volume or weight of storage containers and associated support equipment [11, 18]. 30

2.4 The CAN33 oxygen candle was included as it shows that sodium chlorate has already been implemented in systems that approach the maximum performance of pure (ideal) sodium chlorate. However, due to the rapid release of oxygen, implementing oxygen candles in a power system would require the use of gaseous storage tanks, allowing for a steady flow of oxygen while reducing the system's gravimetric and volumetric storage densities. 44

4.1 Theoretical weight losses were calculated from the stoichiometric oxygen available for decomposition. Differences between theoretical and measured weight loss percentages were most likely due to solid particles being ejected from the TGA pan and removed by the flue gas during testing. The existence of minor side reactions, such as those resulting in the production of chlorine gas, may also have contributed to these differences. 53

4.2 As shown in the literature, small weight percentages of lithium peroxide reduced the 50% DT to around 500°C, with larger percentages of lithium peroxide having negligible effects. 58

4.3 This table summarizes the chemical compositions and testing results from Figure 4-7. 59

4.4 Small particles have higher specific surface areas and are often more active catalysts. 61

4.5 Though useful, TGA results are affected by the various testing conditions. The rate at which samples are heated typically has the largest effect, although even the orientation/arrangement of a sample in the testing pan can impact the results. 63

Chapter 1

Introduction

1.1 Motivation

Unmanned underwater vehicles (UUVs) are increasingly being used due to the number of missions they can accomplish. Whether the mission is military specific, such as Intelligence, Surveillance and Reconnaissance, Mine Countermeasures and Anti-Submarine Warfare or a more general mission involving undersea inspection and maintenance or oceanographic data gathering, UUVs have been identified as potential game changers in these fields. However, without access to atmospheric oxygen, current propulsion systems struggle to provide UUVs with the energy densities that they need. In order to fulfill current and future mission requirements, UUV power systems will need greater endurances and speeds, while also providing enough energy to power increasing hotel loads. One of the most promising areas of research into air independent propulsion (AIP) systems, those that can operate without access to atmospheric oxygen, centers on the different types of fuel cell technologies. A relatively immature technology (when compared to batteries), fuel cell powered systems utilize the oxidation-reduction reaction between hydrogen and oxygen to produce water and electricity. Though still expensive, fuel cells will allow for UUVs to have

power systems that are not only energy dense, but also air independent and easily replenishable. However, to implement fuel cells in underwater vehicle applications, improved methods for reactant storage are needed. Hydrogen and oxygen can be stored as either compressed gases or cryogenic liquids, but these options are less than ideal. Compressed gas storage raises safety concerns due to the high pressures that are required, while cryogenic liquids need large, insulated and often heavy tanks that necessitate constant cooling and venting to handle the accumulation of gaseous products within these systems [1]. Though promising, fuel cells will not meet military, commercial or scientific needs until better reactant storage options are implemented.

In this thesis, I investigated the use of sodium chlorate ($NaClO_3$) as an oxygen storage medium for use in a fuel cell power system. Sodium chlorate is the primary ingredient in most oxygen candles, which are typically used to provide oxygen in emergency situations. Utilizing the thermal decomposition of sodium chlorate into sodium chloride (NaCl) and diatomic oxygen (O_2), oxygen candles are found on commercial aircraft, in mines, submarines and spacecraft [2]. Though the decomposition of sodium chlorate is slightly exothermic, this reaction only proceeds rapidly at high temperatures ($\geq$550°C). This is why oxygen candles typically incorporate small percentages of metal fuels and catalysts. As reported by Shafirovich [2], the combustion of these fuels results in local temperatures inside the candle increasing to around 1000°C. While suitable for emergency situations, once ignited, this type of chemical oxygen generator cannot be stopped or turned off and the contents of the candle will continue to react until they are depleted. Additionally, the highly exothermic nature of the sodium chlorate/metal fuel reaction substantially increases the risk of fire or explosion, especially in the case of contamination with organic-based materials. Though sodium chlorate offers a volumetric oxygen storage density comparable to that of liquid oxygen (LOX) and substantially greater than that of compressed oxygen gas at 70 MPa, the incorporation of metal fuel and resulting self-sustaining

reaction makes it incompatible with a power system that requires the slow, steady and controlled release of oxygen over a period of days, weeks or even months.

1.2 Approach

Given the current state of oxygen storage and generation systems, as it pertains to underwater vehicle applications, several needs must still be met. First, the system must be safe and non-explosive. Second, the storage system must be stable for long periods of time. Finally, the previously mentioned needs must be met without sacrificing the gravimetric and volumetric oxygen storage capabilities of existing methods. To fulfill these requirements, the use of sodium chlorate as an oxygen storage medium was investigated. Mixtures containing cobalt oxide catalysts (Co_3O_4) were studied extensively, however, due to their ability to create explosive mixtures, metal fuels such as iron and tin powders were avoided. As will be discussed in the next chapter, the chosen strategy for generating oxygen was the thermal decomposition of sodium chlorate. Afterwards, the goal was to reproduce and expand upon the relevant literature. This allowed for both quantitative and qualitative information, such as that concerning system operating temperatures, power requirements and mixture preparation, to be obtained. After gaining experience and information concerning catalyzed sodium chlorate mixtures, two concepts for implementing these chemicals in actual systems were investigated. The first concept, which was designed to continuously produce oxygen, relied on a chain powder conveyor. The chain would transport the chemicals into a heated stainless steel tube, which served as a reaction chamber, and would remove the waste products as they decomposed into sodium chloride and oxygen. The second concept relied on a batch process that involved the loading of the sodium chlorate and catalyst powder mixture into a stainless steel reaction chamber, the thermal decomposition of the mixture via heaters external to the reaction cham-

ber, and finally the ejection of the solidified waste materials with a stainless steel piston. Figure 1-1 illustrates the basic steps associated with this batch concept. A fully automated system was not completed, however the most critical steps of the system, those encompassing the loading, chemical decomposition and waste removal, were successfully implemented. This was significant as inadequate waste removal processes currently plague literature oxygen systems utilizing sodium chlorate and similar chemicals.

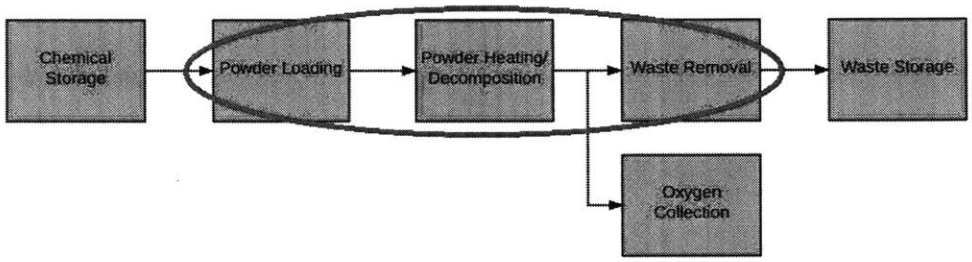

Figure 1-1: Breaking a complex problem down into independent steps allows for the most critical areas to be identified and ultimately addressed.

1.3 Organization

The thesis is organized into six chapters, and three appendices:

- Chapter 1 (this chapter) introduces the problem and its importance and provides the organization of this thesis.
- Chapter 2 provides background material, discusses existing methods of oxygen storage and summarizes much of the foundational literature used to advance this project.
- Chapter 3 describes the equipment and software used to collect data during this project, the chemicals that were handled and appropriate safety measures.
- Chapter 4 describes the analysis that was needed to characterize the thermal behavior of the relevant chemicals. The goal was to also reproduce and ex-

pand upon the literature associated with sodium chlorate by determining what temperatures are needed for various mixtures to decompose rapidly.

- Chapter 5 describes the design and performance of two sodium chlorate oxygen systems.
- Chapter 6 summarizes the results of this thesis and the need for future research into chemical oxygen storage and generation.

THIS PAGE INTENTIONALLY LEFT BLANK

Chapter 2

Background

2.1 Power Systems for Underwater Vehicles

This chapter discusses existing power systems used in underwater vehicles and summarizes various methods of oxygen storage, with an emphasis on chlorate-based oxygen storage methods. Afterwards, the chemistry and literature associated with lithium perchlorate and sodium chlorate, the two most commonly used chlorates for oxygen storage, are presented. Finally, this chapter concludes with a discussion of both hydrogen and oxygen storage selection in fuel cell powered UUVs and which hydrogen storage system should be used with sodium chlorate. This is followed by a short chapter discussing the materials and methods used during this project.

2.1.1 Diesel-electric

A common power system used in underwater vehicles employs diesel engines and batteries. Used since World War I, submarines with these diesel-electric systems run on battery power while underwater. When the batteries need to be charged, they surface/snorkel for air and run the diesel-electric generators. Because surfacing for air made these submarines vulnerable to detection and attack, there were attempts during

the Cold War to implement closed cycle diesel-electric submarines. For example, in 1956 the Soviet Union developed the QUEBEC class submarine which stored liquid oxygen for use in its diesel engines. Additionally, in 1955 the US Navy developed a diesel and battery run midget submarine, dubbed the SSX-1, that stored its required oxygen as hydrogen peroxide [3]. Utilizing the catalyzed decomposition of hydrogen peroxide to provide oxygen for combustion, the diesel engines could be run while under water. Though it achieved acceptable performance, the peroxide oxidant storage was abandoned after an explosion in this system destroyed the entire bow section of the vehicle [3].

2.1.2 Fuel Cells

More recent attempts at implementing air-independent propulsion systems in submarines have involved hybrid systems that incorporate fuel cells. When the operational profile requires peak power for short periods of time, fuel cells are operated in combination with high-performance batteries. Furthermore, if low power is needed for extended periods of time, fuel cells can be operated independently to meet this requirement. Examples of this type of system are found in the German U-212 and U-214 submarines. Equipped with a diesel generator, lead-acid batteries and nine polymer electrolyte membrane (PEM) fuel cells, these submarines are some of the most advanced submarines currently in operation and are advertised as being both quieter and cheaper than their nuclear counterparts [3, 4]. This vehicle, which has a 27 man crew, is shown below in Figure 2-1.

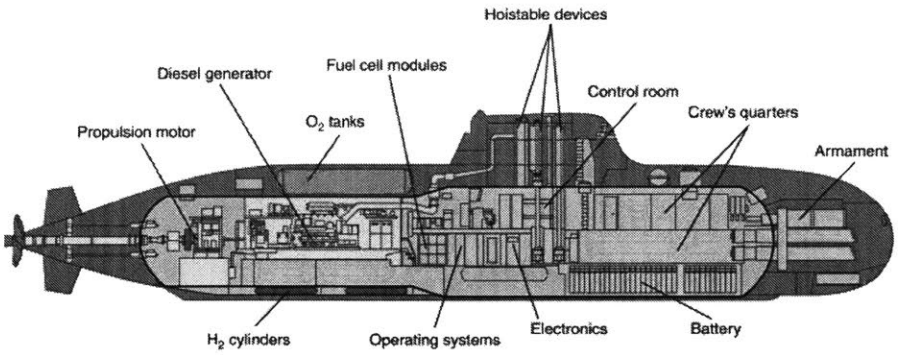

Figure 2-1: The U-212 fuel cell power system, which can generate up to 450 kW, uses cryogenic oxygen storage and metal hydride hydrogen storage, both located outside of the pressure vessel [4, 5].

As fuel cell technologies continue to mature, their use in air-independent power systems will become more commonplace. However, this will require reactant storage methods for both oxygen and hydrogen to be improved upon. Equation 2.1 shows the net overall reaction for a PEM fuel cell which, in addition to waste water, produces heat and useful electricity:

$$2H_2 + O_2 = 2H_2O \tag{2.1}$$

2.1.3 Batteries

Batteries are the most common method of energy storage for unmanned underwater vehicles. For example, a 2004 review of energy sources for 61 different autonomous underwater vehicles showed that 53 of these vehicles used either primary or secondary batteries while five used fuel cells. Two of the vehicles were semi-submersibles that used air-breathing diesel engines and only one of the vehicles operated with a closed cycle diesel engine [6]. For large, manned vehicles, hybrid diesel-electric systems provide favorable energy densities. However, when implemented in smaller vehicles, the volume required for various support equipment decreases the energy density and makes batteries much more attractive [7]. Even though the highest performing lithium-ion batteries are limited in range and elicit safety concerns (due to the

tendency of high energy density batteries to catch fire), batteries will remain the prevalent power source for use in unmanned underwater vehicles until cheaper technologies with greater energy densities can be packaged in small underwater vehicles.

2.2 Oxygen Systems and Storage

2.2.1 Gaseous

The simplest and most obvious method of storing oxygen is as a compressed gas. At normal temperature and pressure (NTP), gaseous oxygen has a density of only 1.33 kg/m^3, meaning it must be stored at high pressures. For example, the AUV Urashima, which is a hybridized vehicle containing both a fuel cell system and lithium-ion batteries, stores its gaseous oxygen at 14.7 MPa [8, 9]. The Urashima and some of its specifications are shown below in Figure 2-2 and Table 2.1.

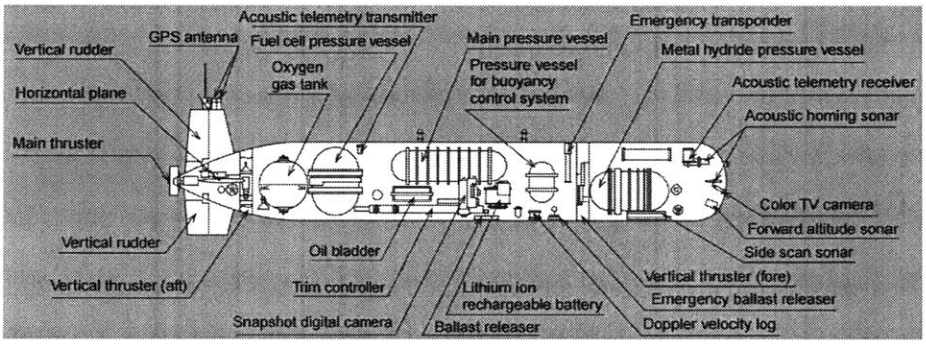

Figure 2-2: The Urashima's fuel cell power system is rated at 4 kW. Its hydrogen is stored in a metal hydride system [10].

Metric	Specifications
Dimensions (m)	10.7 x 1.3 x 1.5
Weight in air (t)	≈ 10
Max. depth (m)	3500
Max. range (km)	300
Cruising Speed (kt)	≈ 3

Table 2.1: The Urashima typically operates autonomously and has a hybrid power system allowing for considerable cruising distances [10].

Similarly, the German DeepC AUV, which also uses a fuel cell and battery hybrid power system, stores its oxygen as a gas at 35 MPa. Though these types of systems can be implemented with minimal balance of plant (BOP), gaseous oxygen raises safety concerns due to its extreme reactivity at high pressures and has both space and weight limitations due to increasing tank wall thicknesses at these high pressures [9, 11].

2.2.2 Liquid

Another proven method of oxygen storage is as a cryogenic liquid. With a boiling point of 90.18 K and a density of 1141 kg/m^3, the oxygen storage capacity of liquid oxygen (LOX) far surpasses that of compressed oxygen gas. Examples of this technology in underwater vehicle applications include the previously mentioned Soviet QUEBEC class and modern day German U-212 submarines, as well as the Japanese Soryu class submarine [4, 12]. Many studies favor the use of liquid oxygen in underwater vehicles, however these systems are often complex due to safety issues with the handling and storage of cryogenic liquids [8, 11]. Additionally, even the best designed liquid oxygen systems carry with them the risk of catastrophic failure due to boiling liquid expanding vapor explosions or BLEVE [13]. Recently, Sierra Lobo, Inc. developed a fuel cell power system for UUVs that uses both liquid oxygen and liquid hydrogen. Advertised as having a specific energy as high as 760 Wh/kg, this power system is much more attractive than either secondary or primary lithium batteries, whose specific energy densities are typically around 120 Wh/kg and 420 Wh/kg, respectively [14]. Below, Figure 2-3 offers a simplified schematic of the Sierra Lobo system and Figure 2-4 shows a CAD model of their power system.

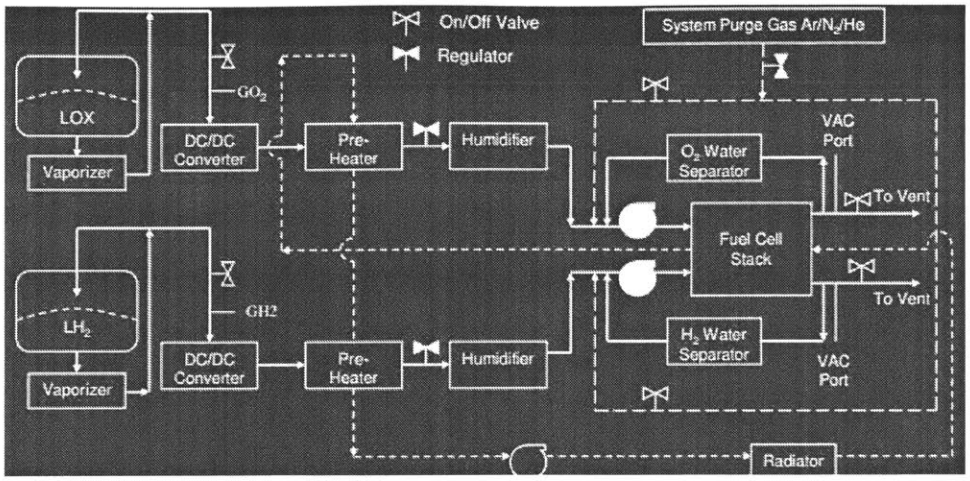

Figure 2-3: The schematic shows that cryogenic storage systems can be rather complicated, requiring support architecture such as pre-heaters, humidifiers and radiators [14].

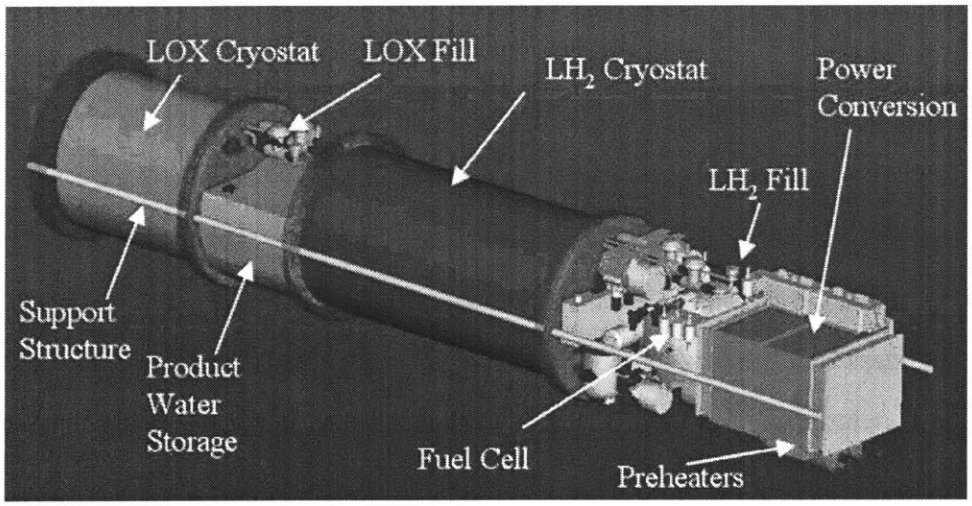

Figure 2-4: Cryogenic storage systems are a proven technology with energy densities greater than secondary silver-zinc and lithium batteries. Advertised as having a $200 refueling cost, Sierra Lobo's power system is more economical than primary lithium ion batteries which, despite similar energy densities, can cost as much as $100,000 per use [14].

2.2.3 Chemical

While oxygen can be stored in its pure form, as either a liquid or a gas, it can also be stored in a chemical that releases oxygen upon decomposition. The most common methods of chemical oxygen storage utilize peroxides/superoxides, chlorates and perchlorates. When hydrogen peroxide (H_2O_2) decomposes, it releases water

vapor and oxygen gas, as per Equation 2.2 below:

$$2H_2O_2 = 2H_2O + O_2 \tag{2.2}$$

An early example of this type of system was the German V80 submarine, which decomposed hydrogen peroxide using a permanganate catalyst. Developed during the 1930s, it reacted diesel fuel with the oxygen to run a high-speed turbine [3]. Figure 2-5 below shows the basic power cycle used by this hydrogen peroxide-based system.

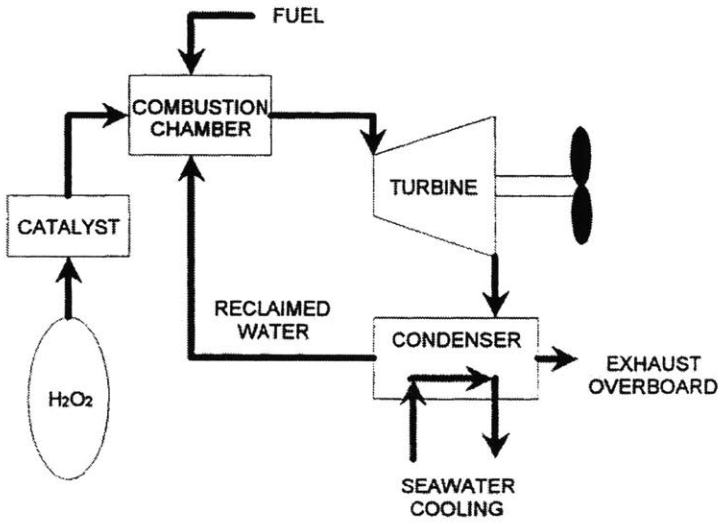

Figure 2-5: This system used 80% concentrated hydrogen peroxide solution. Additional water was added to the combustion chamber to limit the temperature of the reaction and provide more steam to pass through the turbine [15].

Using the same technology, the British, Soviets and US also implemented these systems in submarines. Even though the oxygen contained in the H_2O_2 molecule is relatively easy to liberate, highly-concentrated hydrogen peroxide poses huge safety risks. For example, the Royal Navy's HMS Explorer and HMS Excalibur became known as the HMS Exploder and HMS Excruciator due to the tendency of their hydrogen peroxide systems to explode [16]. Additionally, twelve men died aboard the HMS Sidon after a Mark 12 torpedo, which used hydrogen peroxide as its oxidant

source, malfunctioned and subsequently exploded [16]. Alternatively, chlorates and perchlorates offer safe and stable methods of chemical oxygen storage, especially when compared to hydrogen peroxide. A commonly used chemical, sodium chlorate has a density of 2490 kg/m^3 and is 45.1% oxygen by weight, giving it an oxygen storage density of 1123 kg/m^3. Not accounting for the volume or weight of associated storage equipment for either method, sodium chlorate offers a volumetric oxygen storage density that is only 1.6% less than that of liquid oxygen. Similarly, lithium perchlorate $LiClO_4$ has a density of 2430 kg/m^3, is 60.1% oxygen by weight and has an oxygen storage density of 1460 kg/m^3 (which is 28% greater than that of liquid oxygen) [17]. Though these chemicals can store large amount of oxygen on a volumetric basis, the oxygen is difficult to liberate. Sodium chlorate has an uncatalyzed decomposition point around 480°C, while lithium perchlorate has a decomposition point around 410°C [18]. Because it is impractical to raise the temperature of these salts from ambient temperatures to their decomposition points, they are typically only used as oxygen sources after being mixed with small percentages of catalysts and metal fuels. The catalysts lower the decomposition temperatures by introducing alternate reaction pathways and the metal fuels react with some of the released oxygen to provide the necessary heat. While this type of mixture allows for oxygen to be released with little to no power requirements, the self-sustaining nature of these mixtures also represents a potential hazard. As described by Shafirovich, malfunctioning oxygen generators resulted in "serious fires" on the Mir Space Station and an explosion on the Royal Navy's HMS Tireless in 2007 [2]. Chlorates and perchlorates have the potential to offer safe, stable and dense sources of oxygen storage, but the current methods used to liberate the oxygen eliminates their inherent safety.

2.2.4 Summary of Oxygen Storage Methods

As discussed above, the use of gaseous oxygen storage is limited due to material strength concerns. Despite being relatively easy to implement, space limitations mean that compressed gas storage cannot compete with more oxygen dense storage methods. Furthermore, highly concentrated hydrogen peroxide, also known as high-test peroxide, contains oxygen that is easily liberated. However, this property results in a chemical that is too dangerous to use, as indicated by its abysmal safety record. Similarly, liquid oxygen is difficult to implement due to its stringent safety requirements, poses long-term storage problems and is subject to catastrophic failures due to gas build up in the cryogenic tanks. Moreover, refueling of these types of systems is challenging, as support vehicles must carry with them the equipment necessary for storage and/or production of cryogenic liquids. Though there is a trade-off to be made between ease of access of the stored oxygen and the stability/safety of the chemical mixture, chlorate-based oxygen storage is both promising and proven. Table 2.2 provides a comparison of the oxygen storage metrics of the discussed methods. Note that while sodium chlorate competes with the storage ability of liquid oxygen, it suffers a weight penalty due to the added sodium chloride. Also, the relative safety metric is based off of this author's review of the literature and associated failures of these types of systems.

Substance	Density, kg/m^3	kg O_2/kg cmpd	Kg O_2/m^3	Relative Safety
GOX (@ 48.3 MPa)	540	1	540	3
H_2O_2	1387	.42	583	4
$NaClO_3$	2490	.45	1123	1
LOX (@ -183 C)	1141	1	1141	2

Table 2.2: Sodium chlorate stores nearly as much oxygen as LOX but, when used in formulations without metal fuels, is inherently safer [11, 18].

Below, Table 2.3 includes the oxygen storage densities, melting temperatures and decomposition temperatures of various chlorates and perchlorates that could be used

for oxygen generation. Sodium chlorate is most commonly used due to its relatively low cost and the abundance of associated literature, however this literature review also discusses the use of lithium perchlorate and lithium chlorate. Due to their high oxygen content and relative safety, lithium perchlorate and lithium chlorate have also been studied extensively for use in underwater oxygen generation systems.

Substance	Formula	kg O_2/kg cmpd	kg O_2/m^3	T_{melt} (°C)	T_{decomp}(°C)
Lithium Perchlorate	$LiClO_4$	0.60	1450	247	410
Lithium Chlorate	$LiClO_3$	0.53	1420	129	270
Sodium Perchlorate	$NaClO_4$	0.52	1310	471	482
Potassium Perchlorate	$KClO_4$	0.46	1160	585	400
Sodium Chlorate	$NaClO_3$	0.45	1123	248	478
Potassium Chlorate	$KClO_3$	0.39	910	357	400
LOX (@ -183°C)	O_2	1	1141	-	-

Table 2.3: LOX has the best gravimetric oxygen storage capacity, due to it being a pure substance, but the chemical storage methods can provide better volumetric oxygen storage. Note that this comparison does not include the volume or weight of storage containers and associated support equipment [11, 18].

2.3 Chlorate-based Oxygen Storage

This section discusses various chlorate-based oxygen storage and generation methods and previous work done at MIT. Aside from solid storage, chlorates have also been implemented in systems where they are stored in their molten form and in aqueous solutions.

2.3.1 Solid Chlorate Storage

Chlorates are used as the primary ingredient in oxygen candles. Also known as self contained oxygen generators, they have been used for decades in emergency situations [19]. Figure 2-6 below shows the basic assembly of an oxygen candle. The mixture typically consists of a chlorate, a metal fuel additive, such as iron powder, a catalyst to reduce the chlorate's decomposition temperature, an additive that scavenges chlorine-

containing compounds, and a binder, such as glass fiber or steel wool, to improve the structural integrity of the candle. The mixture is usually cast, pressed or hot-pressed into the desired shape. The burning of the ignition cone, which contains a high percentage of metal fuel, can be achieved through the use of a flash power train or heated metal coil [18]. Once initiated, the exothermic nature of the mixture ensures self-sustained combustion front propagation.

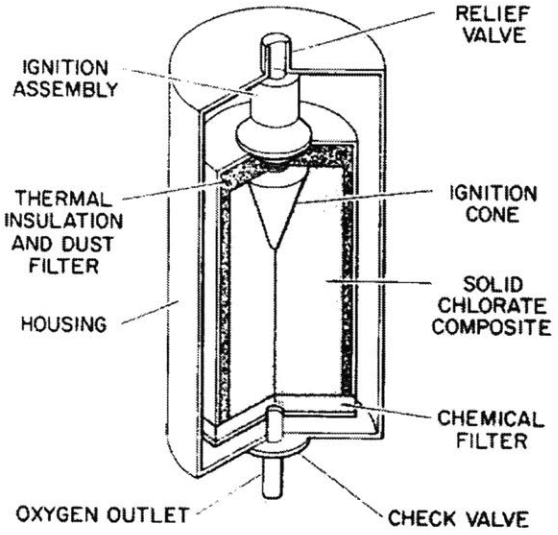

Figure 2-6: Oxygen candles are only used once, typically during emergency situations, and are designed to be self-sustaining. The insulation and housing help maintain the high internal temperatures needed for complete combustion while also preventing damage to surrounding equipment.

Another example of how chlorates have been used while in their solid form is in the work done at Penn State's Applied Research Laboratory (ARL). Due to its high oxygen content compared to liquid and gaseous oxygen (as previously discussed), they chose to use lithium perchlorate. Using compressed air, they forced a solid slug of lithium perchlorate into a sanding screen to create a powder. The powder was then fed into a distributor, which relied on an augur to feed the lithium perchlorate into the reaction vessel [20]. Figure 2-7 shows the basic layout of their oxygen reactor, not including the powder generator.

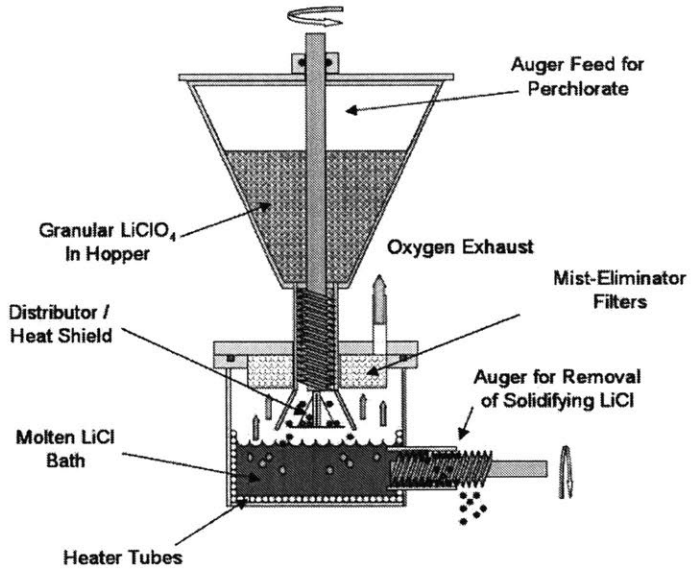

Figure 2-7: In order to prevent lithium perchlorate from prematurely melting and causing the system to fail, the engineers added heat shielding to the powder distributor. One advantage of using lithium perchlorate instead of sodium chlorate is that the lithium chloride byproduct melts at 605°C, well below the 800°C required to melt sodium chloride, making it easier to transport.

Lithium perchlorate begins decomposing between 316°C and 410°C, however the rate of reaction in this range is quite slow [20, 21]. In order to rapidly decompose the lithium perchlorate into oxygen gas and lithium chloride, the researchers at ARL maintained the reaction vessel around 650°C utilizing steam from a parallel steam turbine subsystem and electrical heaters. Continuous oxygen generation also meant that the lithium chloride waste had to be continuously removed from the vessel. As seen in the figure above, an augur was initially used to remove the waste products. However, it struggled to accurately transport liquid waste products and would seize if the molten salt cooled enough to become solid. Ultimately, the researchers settled on a heated pintle valve that allowed for the continuous removal of molten waste [20].

2.3.2 Molten Chlorate Storage

An earlier system designed by ARL instead stored lithium perchlorate between 288°C and 316°C. This range is above its melting point of 247°C and allows for only

minimal decomposition. The molten lithium perchlorate was pumped into the reaction vessel and then sprayed against a heated surface, which was held at approximately 650°C [21]. Figure 2-8 below illustrates the basic concept:

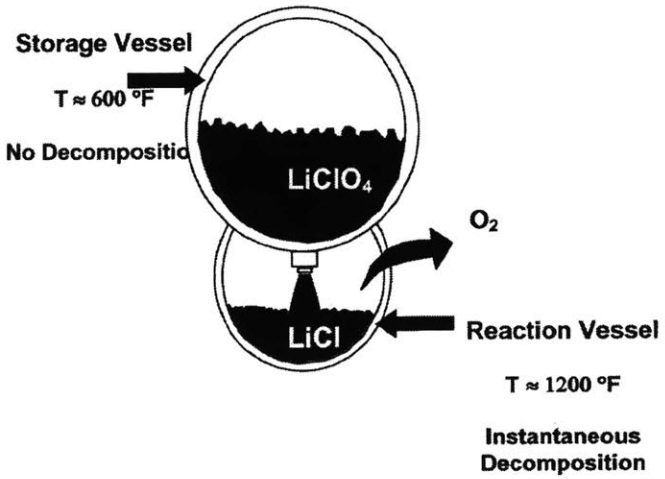

Figure 2-8: Storing lithium perchlorate as a liquid simplifies transport into the reaction chamber; however, premature decomposition around the injection port can result in system failure. Lithium chloride waste has a higher melting point than lithium perchlorate, meaning it will form as a solid and eventually plug the port.

Though this system seemed simple in implementation, it struggled with several significant and potentially dangerous issues inherent in its design. The first issue with the two-chamber concept was the storage of waste lithium chloride in the reaction vessel. Without removal, the volume of the reaction vessel would have to be sized to accommodate the waste from all of the lithium perchlorate in the storage vessel. This volume requirement would result in significant losses in both gravimetric and volumetric energy densities, making this type of system unattractive in space-limited applications. Though this issue could be addressed by introducing a heated waste removal valve, as was done in the previously described system from ARL, the frequent plugging of both inlet and exhaust lines into the reaction chamber posed a much more dangerous issue. After Test 1 of the system, the researchers found that the diameter of the oxygen exhaust port had been reduced from 0.281 to 0.23 inches, corresponding to a 33% reduction in the area of the exhaust port. During Test 2, a faulty heater

in-between the storage and reaction vessels allowed for cold spot in the transfer line, freezing the molten lithium perchlorate and completely jamming the system. During Tests 3 and 4, some of the lithium perchlorate prematurely decomposed in the reaction vessel injection port. Because lithium chloride has a melting point of 605°C, well above the temperature of the storage vessel and injection port, the lithium chloride froze and jammed the system. Finally, similar to Test 1, Test 5 suffered from lithium chloride buildup reducing the area of the oxygen exhaust port from 0.281 inches to 0.15 inches, corresponding to a 72% reduction in area [21]. Even though this system was a prototype and not the final design, plugging of valves and ports throughout the system could result in potentially catastrophic failures. This could include an inability to restart the system after unexpected drops in temperature or rapid pressurization causing ruptures in the reaction vessel or connected piping.

2.3.3 Aqueous Chlorate Storage

Lithium chlorate ($LiClO_3$), which is 53% by weight oxygen and begins decomposing around 270°C, is attractive as an oxygen source [18]. It has been described as being very deliquescent and will absorb water from the surrounding atmosphere until it dissolves in the absorbed water [22]. This property makes it unattractive for long term storage as a solid. However, due to its high solubility, aqueous lithium chlorate has shown promise for use in an oxygen storage and generation system. While sodium chlorate and lithium perchlorate have solubilities in water of 106 g/100 mL and 60 g/100 mL at 25°C [23, 24], respectively, lithium chlorate has a solubility in water of 314 g/100 mL at 18°C [25], making it one of the most soluble inorganic salts. For example, a saturated solution at 20°C contains more available oxygen on a volumetric basis than compressed oxygen gas at 10,000 psi (69 MPa) [25]. This property led scientists at API Engineering, who have been developing oxygen systems for solid oxide fuel cell (SOFC) underwater power systems, to design an oxygen storage and

generation system using aqueous lithium chlorate. Their system used the following batch process:

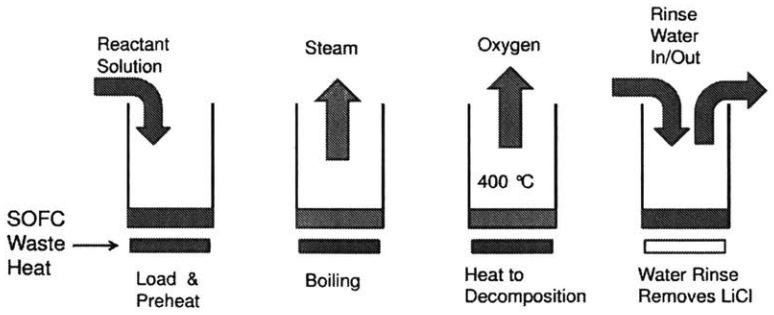

Figure 2-9: Decomposing aqueous lithium chlorate first requires that the water be evaporated. A water rinse is also used to remove the solid lithium chloride waste from the reaction chamber. As these processes significantly increase this system's energy requirements, the engineers at API designed an integrated system that utilizes fuel cell waste heat [26].

After loading the lithium chlorate solution into the reaction chamber, the water is boiled off. The remaining lithium chlorate solid is heated to around 400°C, where it decomposes rapidly. The lithium chloride waste is rinsed out and the aforementioned sequence is repeated. Potential benefits from this type of system include added safety and easy handling/control associated with liquid transport. However, the water necessarily adds weight, reducing the gravimetric oxygen storage density, and the energy required to boil the water reduces the energy density of the total system. For example, assuming a solution at room temperature (20°C), the heat required to remove the water accounts for 71% of the total heat required to operate the oxygen system [25]. To meet the added power requirements, the scientists at API assumed that a final system would utilize waste heat, from either a combustion power cycle or high temperature fuel cell [25].

2.3.4 Previous Work Done at MIT

Previous work done at MIT focused on using the thermal decomposition of sodium chlorate to produce oxygen for future use in a fuel cell powered underwater vehicle.

Figure 2-10 below illustrates the basic idea that was investigated. The goal was to use conventional powder conveying methods to drag powderized sodium chlorate through a heated region/defacto reaction chamber. The sodium chlorate would be heated to decomposition and the oxygen would be released through an exhaust port. The remaining sodium chloride waste products would then be returned to the initial storage tank where a membrane would separate the waste products from the unreacted sodium chlorate [27].

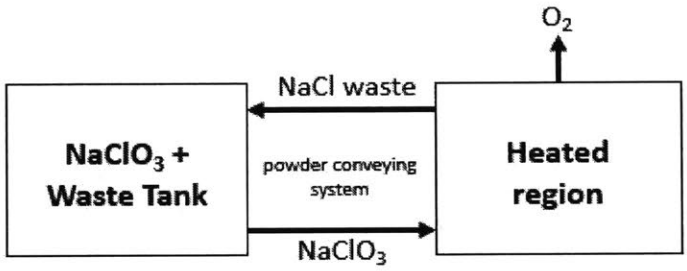

Figure 2-10: Returning the waste products to the reactant storage container would improve this system's volumetric and gravimetric oxygen storage densities by eliminating the space and weight occupied by a separate waste container [27].

Returning the waste products to the reactant storage tank would decrease the weight and volume of this oxygen system by removing the need for a separate waste storage tank and would simplify the refueling/replenishment process. After reviewing various powder conveying technologies, the students at MIT designed a chain type tubular drag conveyor. Figure 2-11 shows a schematic of the bead chain conveyor system and Figure 2-12 shows the corresponding prototype. Note that Figure 2-12 does not include the stainless steel tank that was used to store the chemicals and mechanical components and that a waste-reactant separator had not yet been implemented.

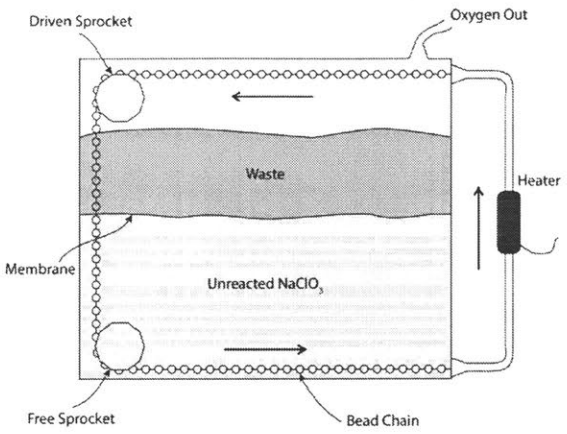

Figure 2-11: This reactor was designed to store some of the released oxygen gas, decreasing the risk from over-pressurization and allowing for variable oxygen demand [27].

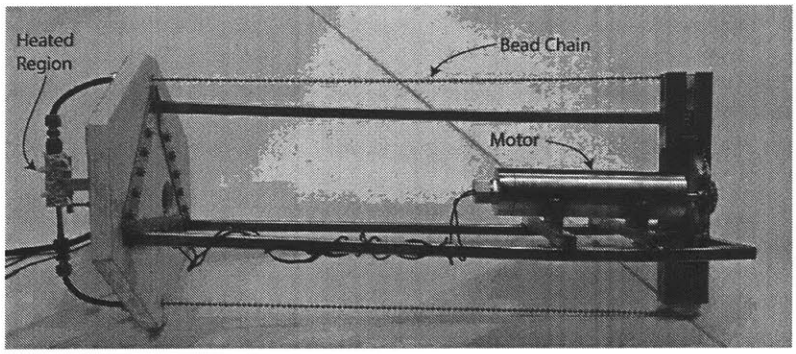

Figure 2-12: Most of the components in this system were made from stainless steel. The authors recommended future systems utilize lighter oxygen compatible materials, thereby increasing the system's gravimetric storage density [27].

This system was designed to provide enough oxygen for a Horizon 200 W PEM fuel cell which, at maximum output, requires 2.6 L/min of hydrogen gas. Assuming hydrogen gas at the maximum stack temperature of 65°C and 101.3 kPa, this equates to an oxygen flow rate of 1.13 L/min (at NTP conditions) and a sodium chlorate decomposition rate of 3.3 g/min. A major issue faced by this system and later iterations was the power consumption. Initial tests using a single 45 W heater decomposed an average of 1.4 g/min of sodium chlorate while tests using two 45 W heaters decomposed an average of 4.8 g/min [28]. Though the required rate of oxygen was exceeded during the hour long test, a power consumption of 90 W (plus the 12 W required to

power the bead chain powder conveyor) was unacceptably high when designing for a fuel cell power system that produces 200 W. Another issue with this system was the tendency of the bead chain to stretch by as much as 20% and eventually yield due to the high temperature loading. A trade-off made by the students working on this project was to use pure sodium chlorate instead of a sodium chlorate and cobalt oxide catalyst mixture. Cobalt oxide is both toxic and carcinogenic, however the lack of catalyst greatly increased the temperature and power requirements of this oxygen system.

Though this system had significant power requirements, further refinement could allow it to provide a safe, stable and controllable oxygen generation method. As such, the reproduction and analysis of work surrounding the bead chain conveyor system was a part of this thesis.

2.4 Chemistry

Chemicals initially considered for further study included lithium chlorate, lithium perchlorate and sodium chlorate. However, as previously discussed, lithium chlorate is only practical when stored in aqueous solution. Due to the heat input and added components necessary to boil, condense and store the waste water, lithium chlorate was removed from consideration. The rest of this section discusses literature relevant to the decomposition of lithium perchlorate and sodium chlorate and the choice to continue working with sodium chlorate.

2.4.1 Decomposition of Lithium Perchlorate

Lithium perchlorate primarily decomposes according to the following over-all reaction:

$$LiClO_4(s) = LiCl(s) + 2O_2(g) \tag{2.3}$$

Lithium perchlorate has been reported to decompose around 410°C (Table 2.3), but rapid decomposition does not occur until about 475°C. Below, Figure 2-13 shows the thermal behavior of pure lithium perchlorate. During this experiment, a 0.8131 g sample of lithium perchlorate was heated with a steadily rising temperature rate of 8.5°C/min. Performed in an inert argon atmosphere, the weight of the sample was continuously measured until complete decomposition had been achieved [17]. Called thermogravimetric analysis (TGA), this technique is typically used to characterize the thermal behavior of substances.

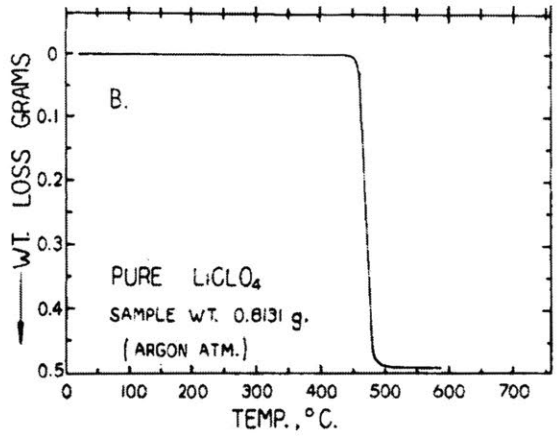

Figure 2-13: Thermogravimetric analysis showed that approximately 50% of the available oxygen had decomposed at 475°C. This was accompanied by exothermic behavior between 460°C and 530°C, observed during differential thermal analysis [17].

Some decomposition and corresponding oxygen evolution is present around 410°C, with Figure 2-13 suggesting that this reaction only proceeds quickly at higher temperatures. Because the power demanded by an oxygen system utilizing chlorates and perchlorates is dependent on the decomposition temperatures that must be achieved, lowering those temperatures is critical. According to the literature, metal oxides such as manganese oxide (MnO_2 and Mn_2O_3), chromium oxide (Cr_2O_3) and cobalt oxide (Co_2O_3) have all shown promise as catalysts for the thermal decomposition of lithium perchlorate [17, 29]. For example, Markowitz showed that a mixture of lithium perchlorate containing 5% by weight manganese oxide decomposed rapidly around 450°C.

Burcat and Steinberg confirmed this result and also showed that chromium oxide allows for rapid decomposition around 400°C while cobalt oxide allows for rapid decomposition around 350°C. Though these results were promising, the chromium and cobalt oxide catalysts were between 20% and 25% by weight of the tested mixtures[1] reducing the amount of available oxygen. Other reported catalysts for the decomposition of lithium perchlorate include lithium oxide (Li_2O) and lithium chloride (LiCl), however this author was unable to find specific details such as the degree to which the decomposition temperatures had been reduced and specific molar or weight percentages of the catalysts [21].

2.4.2 Decomposition of Sodium Chlorate

Sodium chlorate primarily decomposes according to the following over-all reaction:

$$2NaClO_3(s) = 2NaCl(s) + 3O_2(g) \tag{2.4}$$

Several minor side reactions have been proposed, one of which results in the production of chlorine gas which, at least in breathing applications, is somewhat undesirable [17, 18]:

$$4NaClO_3(s) = 2Na_2O(s) + 5O_2(g) + 2Cl_2(g) \tag{2.5}$$

According to the literature, sodium chlorate has a decomposition temperature of 478°C (Table 2.3). However, Figure 2-14 shows that significant decomposition only occurs between about 500°C and 600°C.

[1]Burcat and Steinberg used lithium perchlorate trihydrate instead of pure lithium perchlorate [29]. When determining the catalyst weight percent of their mixtures, this author first subtracted the weight of the contained water.

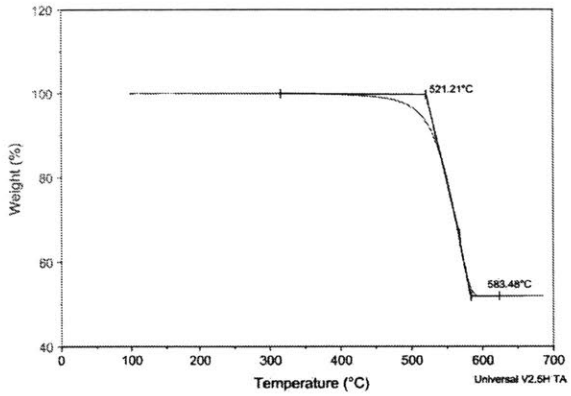

Figure 2-14: The authors heated 9.8 mg of sodium chlorate at 10°C/min. Results showed onset and final decomposition temperatures of 521°C and 583°C, respectively [2].

Catalysts for the decomposition of sodium chlorate include cobalt oxide (Co_3O_4), cobalt chloride ($CoCl_2$), barium peroxide (BaO_2) and lithium peroxide (Li_2O_2). Cobalt oxide is the most promising catalyst for the decomposition of sodium chlorate, as it has been shown to reduce required temperatures by 200°C to 300°C, while barium peroxide and lithium peroxide are only mild catalysts and are primarily used to suppress chlorine production resulting from side reactions [2, 30]. Figure 2-15 below shows the effect of both microscale and nanoscale cobalt oxide catalysts on the decomposition of sodium chlorate. In the case of the nanoscale catalyst, decomposition started before the mixture had fully liquefied.

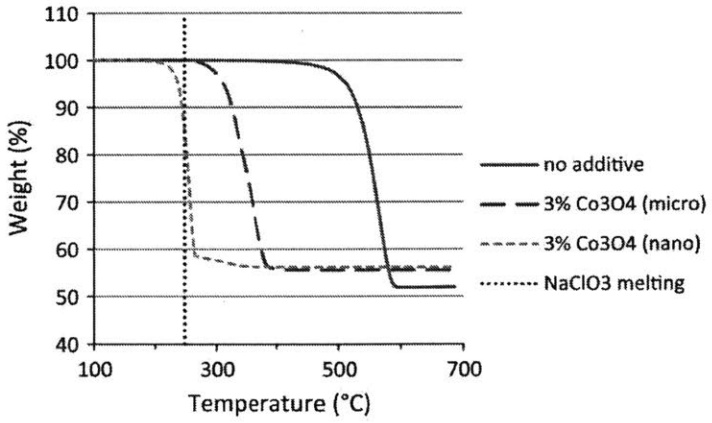

Figure 2-15: The results showed that nanoscale cobalt oxide catalyst can result in significant decomposition while sodium chlorate is still in the solid phase [2].

Though lithium perchlorate contains approximately 23% more oxygen than sodium chlorate (1450 kg O_2/m^3 vs 1123 kg O_2/m^3), much of the literature concerning the catalytic decomposition of lithium perchlorate lacks detail. Furthermore, when details such as specific weight percentages and relevant temperatures are given, the literature shows that large amounts of catalyst (>20% by weight) are needed to achieve decomposition temperatures around 350°C. In contrast, there exists an an abundance of literature concerning the catalytic decomposition of sodium chlorate. For example, decomposition temperatures between 245°C and 350°C are achievable with catalyst weight percentages as low 1% [30, 31], making sodium chlorate competitive with lithium perchlorate, despite its reduced oxygen content. And while cost is less important when performance is the primary goal, a review of similar chemical grades and purities showed that lithium perchlorate is between two and twenty times as expensive as sodium chlorate [32, 33]. As such, sodium chlorate was chosen as the oxygen source for this research.

2.5 Hydrogen Storage Selection

2.5.1 Gravimetric and Volumetric Energy Densities

The gravimetric and volumetric oxygen storage densities of various methods have been discussed above. However, the final selection of an oxygen storage system for fuel cell powered unmanned underwater vehicles requires that the hydrogen storage system also be taken into account. For example, these systems should be sized in relation to one another, as an oxygen system that provides for 10 days of operation would go to waste if its hydrogen system only lasted 5 days. Furthermore, the average density of the power system should be near the density of seawater, as a typical requirement for unmanned underwater vehicles is that they be neutrally buoyant. If a proposed vehicle is too heavy, components from another part of the vehicle must be

removed, thereby reducing its capabilities. Similarly, if a vehicle is too light, ballast must be added. This is wasteful, as the ballast takes up some volume and its weight could have been used to incorporate additional components. To design a neutrally buoyant vehicle, one approach is to ensure that its subsystems each approach neutral buoyancy. For a fuel cell powered vehicle, this means that the chosen hydrogen system can have a relatively large mass or require a lot of space, if it is paired with an oxygen system that has a relatively small mass or occupies a small volume. Equations 2.6 and 2.7 were used to calculate the volumetric energy density (kWh/L) and specific energy density (kWh/kg) of different hydrogen and oxygen storage combinations and identify which method of hydrogen storage should be paired with a sodium chlorate oxygen storage system. The development of these equations, which were used by Davies and Moore in their 2006 UUV Technology Assessment [9], can be found in Appendix A.1. Even though hydrogen is generally considered to be the energy carrier/fuel, the stoichiometric redox reaction (Equation 2.1) allows for oxygen and product water storage to be accounted for. The volumetric energy density calculation includes a product water term, based on the assumption that waste water would be stored inside a potential UUV and not ejected from the vehicle. Using the lower heating value of hydrogen (241.83 kJ/mol$_{H_2}$) and ignoring the volume and weight of an empty water storage tank, this term reduces to 3.73 kWh/L (see Appendix A.1). However, the gravimetric energy density calculation did not include a product water term, as conservation of mass ensures the gain in mass from waste water is balanced by mass losses in the hydrogen and oxygen storage systems.

$$ED_{SS} = \eta_{FC} \cdot \frac{1}{\frac{1}{ED_{H_2}} + \frac{1}{ED_{O_2}} + \frac{1}{ED_{H_2O}}} \tag{2.6}$$

$$SE_{SS} = \eta_{FC} \cdot \frac{SE_{H_2} SE_{O_2}}{SE_{H_2} + SE_{O_2}} \tag{2.7}$$

2.5.2 Hydrogen and Oxygen Storage Combinations

Table 2.4 shows the considered hydrogen and oxygen storage systems, their respective gravimetric and volumetric energy densities and the various assumptions that went into these calculations. In general, oxygen and hydrogen systems that store their reactants in chemical compounds achieve increased volumetric energy densities, but suffer from decreased gravimetric energy densities, when compared to systems that store their reactants as pure substances.

Table of Assumptions

Hydrogen Storage

	Method	ED (kWh/L)	SE (kWh/kg)	System Density (kg/L)	Details/Assumptions
1	Lithium Hydride Slurry	1.98	2.15	0.92	60 wt. % LiH/ 40 wt. % light mineral oil. LiH reacts with water to produce lithium hydroxide and hydrogen gas. Considers weight of hydride/mineral oil slurry and water required for reaction. Does not include mass or volume of waste products and operating/storage equipment.
2	Hydrogen Gas (@5076 psi)	0.61	1.78	0.34	Luxfer carbon composite cylinder. Considers mass and volume of tank and contents.
3	Aluminum	1.57	1.24	1.27	System currently in development at MIT. Aluminum reacts with water to produce hydrogen, aluminum hydroxide and heat. Considers weight of aluminum and reactant water. Does not include mass or volume of waste products and operating/storage equipment.
4	Liquid Hydrogen (@-253 C)	1.23	1.72	0.72	Stainless steel cryogenic tank used in HydroGen3 fuel cell vehicle. Considers weight and volume of tank and contents.

Oxygen Storage

	Method	ED (kWh/L)	SE (kWh/kg)	System Density (kg/L)	Details/Assumptions
a	90% Hydrogen Peroxide	2.09	1.61	1.30	Values obtained from UUV Technology Assessment. Assumptions unknown. Included for comparison purposes.
b	CAN33 Oxygen Candle	3.08	1.53	2.01	Sodium chlorate oxygen candle. Volume and mass of candle and initiation mechanism included.
c	Oxygen Gas (@3000 psi)	0.84	1.56	0.54	Luxfer carbon composite Cylinder. Considers mass and volume of tank and contents.
d	Liquid Oxygen (@-183 C)	2.78	3.30	0.84	Sierra Lobo LOX system. Includes mass and volume of inner vessel, vacuum jacket, supports, insulation, piping, heat exchangers and contents.
e	Ideal NaClO3	4.71	1.89	2.49	Considers only the mass and volume of pure Sodium Chlorate. Does not include operating/storage equipment.
f	Ideal LiClO4	6.11	2.53	2.42	Considers only the mass and volume of pure Lithium Perchlorate. Does not include operating/storage equipment.

Table 2.4: The CAN33 oxygen candle was included as it shows that sodium chlorate has already been implemented in systems that approach the maximum performance of pure (ideal) sodium chlorate. However, due to the rapid release of oxygen, implementing oxygen candles in a power system would require the use of gaseous storage tanks, allowing for a steady flow of oxygen while reducing the system's gravimetric and volumetric storage densities.

Figure 2-16 below shows the volumetric and gravimetric energy densities of var-

ious oxygen/hydrogen storage combinations, with systems to the left of the dashed line being weight limited (negatively buoyant) and systems the right of the dashed line being volume limited (positively buoyant). The maximum performance of systems using pure sodium chlorate and lithium perchlorate as oxygen storage methods (i.e. not including the power required to extract the stored oxygen) are included as they identify the upper bound of performance offered by those types of systems. Each combination is designated by a number/letter combination, with numbers corresponding to the type of hydrogen system and letters corresponding to the type of oxygen system (see Table 2.4). To give more realistic energy density values, a fuel cell efficiency of 60% was assumed. Furthermore, the performance of various battery technologies are included to illustrate the potential that fuel cell systems have for unmanned underwater vehicles.

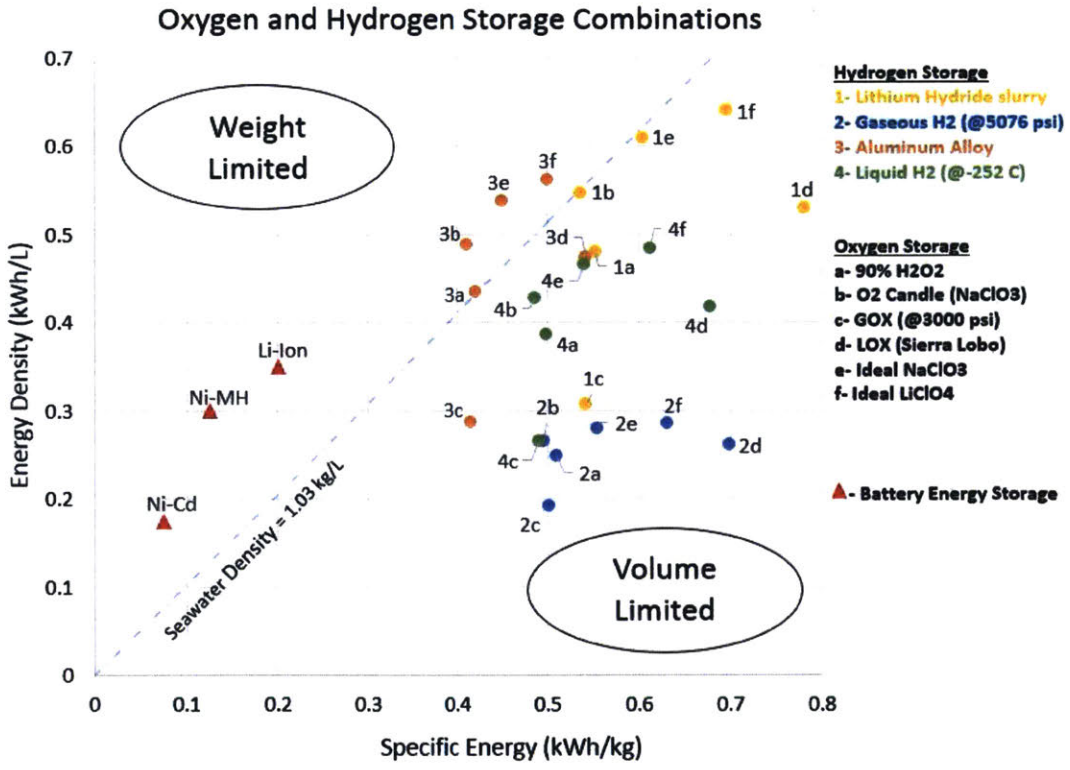

Figure 2-16: Ideal power systems offer high volumetric and gravimetric energy densities, while maintaining average densities near that of seawater. Underwater vehicles can deviate somewhat from neutral buoyancy through the use of drag-inducing lifting surfaces.

Figure 2-16 shows that a sodium chlorate oxygen system should be paired with a lithium hydride hydrogen storage system, as this combination would result in a highly energy dense system that is closest to being neutrally buoyant. However, once prices are considered, a hydrogen storage system that uses aluminum (≈2/kg), becomes much more attractive than a lithium hydride hydrogen storage system (≈800/kg) [32]. And while water contamination is an issue for both of these systems, the lithium hydride slurry is only stable for a few weeks, while the aluminum system is stable indefinitely [34, 35]. Gaseous and liquid hydrogen storage are both proven technologies, but these systems are volumetrically limited and require stringent safety procedures and precautions, especially during refueling processes.

Chapter 3

Materials and Methods

This chapter briefly describes the materials and measurement equipment used during this project, the software used to analyze collected data and the material safety and storage requirements dictated by MIT's Environmental Health and Safety Department.

3.1 Equipment and Software

Equipment used during this project include the TA Instruments Discovery TGA, which was used to characterize decomposition temperatures of different chemical mixtures, the Jeol 6010LA SEM, which was used to characterize particle sizes and assess mixture preparation techniques, and the Micromeritics ASAP 2020, which was used to measure/confirm catalyst surface areas using BET analysis. The TGA tests, unless otherwise noted, were conducted in nitrogen gas with a 10 ml/min flow rate through the balance chamber and a 25 ml/min flow rate through the furnace. The samples, weighing 10±2 mg, were heated at 20°C/min in a high temperature platinum pan. Samples for BET testing were heated at 150°C for 1 hour under vacuum to drive off any volatile materials adsorbed on the surface of the catalyst. Nitrogen was used as the adsorbent gas for this testing. Binary and triple mixtures of sodium chlorate,

cobalt oxide and lithium peroxide were mixed with a porcelain mortar and pestle for 5 minutes. Software used includes Arduino for thermocouple data collection and servo/piston position control, EES and Matlab for equation solving and plotting, TRIOS for TGA data collection and Solidworks for prototype modeling.

3.2 Chemicals

The following chemicals were obtained from Sigma-Aldrich:

- Sodium chlorate powder ($NaClO_3$), purity: $\geq$99%
- Cobalt oxide (Co_3O_4), particle size:<10 μm
- Cobalt oxide (Co_3O_4), particle size:<50 nm, purity: $\geq$99.5% (trace metal basis)
- Lithium peroxide powder (Li_2O_2), purity: <90% (technical grade)

3.3 Storage and Safety

Before handling the above-mentioned chemicals, the Mechanical Engineering department's Environmental Health and Safety (EHS) coordinator as well as MIT EHS were consulted. When handling chemicals, which were stored in secure locations away from heat and combustible materials, appropriate personal protective equipment was used at all times. This included the use of disposable nitrile gloves (double-gloved), safety glasses, a lab coat and a NIOSH certified N100 respirator. Chemical containers were opened and the chemicals were used while in a fume hood. Waste materials were double-bagged in plastic storage bags obtained from the local VWR supplier and placed in secondary containers for disposal. At the recommendation of the Mechanical Engineering EHS coordinator, water was added to storage bags with dry waste materials in order to increase safety by preventing dust formation.

Chapter 4

Thermal Analysis and Mixture Preparation

4.1 Thermal Analysis of $NaClO_3$

This section begins with an estimate of the power required for the decomposition of different sodium chlorate and lithium perchlorate mixtures found in the literature. Afterwards, comparisons between mixtures with cobalt oxide catalysts of different particle sizes and between mixtures with different catalyst percentages are offered. After deciding upon a specific particle size and weight percentage for the cobalt oxide catalyst, this section includes the identification of an ideal system operating temperature. This section concludes with an analysis of the byproducts from the thermal decomposition of catalyzed sodium chlorate and the effects of lithium peroxide, a chlorine scavenger and mild catalyst, on the decomposition of sodium chlorate.

4.1.1 Power Requirements

Equation 4.1, shown below, was used to estimate the power required for oxygen generation. $\dot{Q}$ is the required power input, $\dot{n}_{naclo3}$ and $\dot{n}_{co3o4}$ are the respective molar

flow rates of sodium chlorate and cobalt oxide catalyst, Δh_{fus} is the heat of fusion for sodium chlorate, $c_{p,s}$ and $c_{p,l}$ are the specific heats of sodium chlorate in its solid and liquid states and $c_{p,co3o4}$ is the specific heat of the catalyst. Though useful for the comparison of various mixtures, this estimate does not account for the exothermic heat release during decomposition or geometry and insulation dependent heat losses. See Appendix B for a listing of the property values used in this analysis.

$$\dot{Q} = \dot{n}_{naclo3}\Big(\int_{T_{low}}^{T_m} c_{p,s}dT + \Delta h_{fus} + \int_{T_m}^{T_d} c_{p,l}dT\Big) + \dot{n}_{co3o4}\Big(\int_{T_{low}}^{T_d} c_{p,co3o4}dT\Big) \qquad (4.1)$$

A required oxygen flow rate of 1.5 g/min or 1.13 L/min at NTP conditions was assumed (based on the hydrogen requirements of a 200 W PEM fuel cell), and used to calculate the required decomposition rate of sodium chlorate. This equation accounts for the heat required to raise the temperature of sodium chlorate and an included catalyst from room temperature (25°C) to sodium chlorate's decomposition temperature. Because reported decomposition temperatures vary greatly in the literature, the decomposition temperature for this estimate was assumed to be the temperature at which 50% of the material available for decomposition has reacted during TGA testing. The use of the 50% decomposition temperature (50% DT) for comparison of different sodium chlorate mixtures, which was used by Zhang, Kshirsagar and Cannon in their analysis of lithium peroxide and sodium chlorate mixtures [30], was also used in this research to describe the temperature at which rapid decomposition occurs. There is some variability in the results from TGA tests, however the 50% DT offered a consistent method of determining the decomposition temperature. Equation 4.1 was used to compare the power requirements for both catalyzed and uncatalyzed sodium chlorate and lithium perchlorate mixtures and shows the importance of reducing the required decomposition temperature. The results, shown below in Figure 4-1, indicate that using 3% by weight nanoparticle cobalt oxide catalyst, sodium chlorate can

potentially outperform lithium perchlorate as an oxygen storage medium.

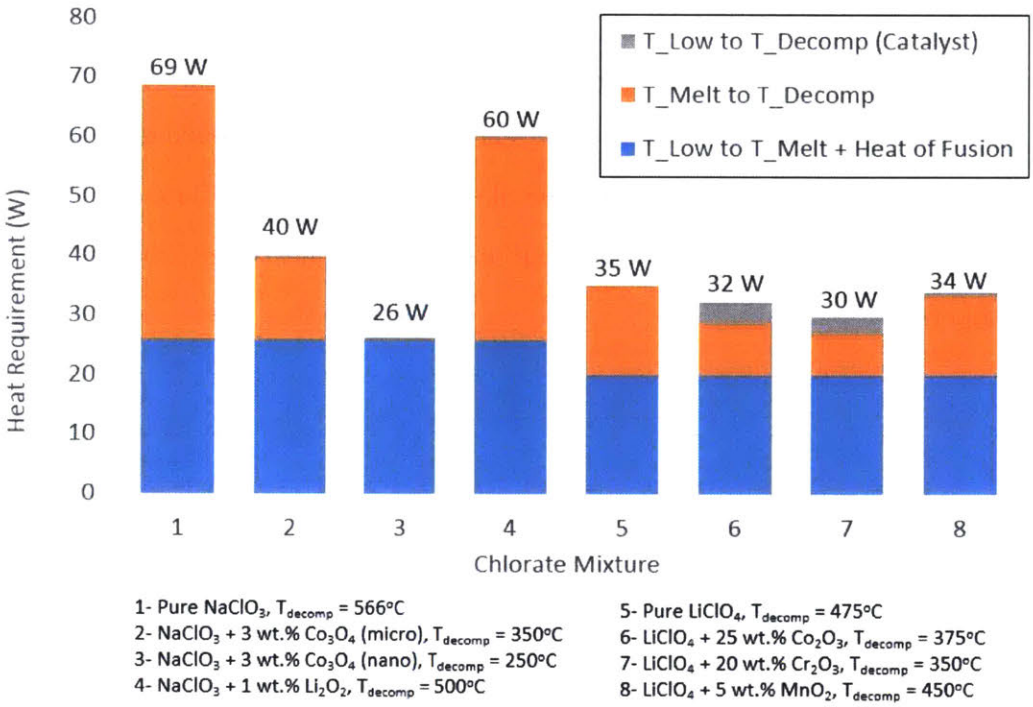

Figure 4-1: Decomposing near its melting point significantly reduces heating requirements for the 3% by weight nanoparticle cobalt oxide mixture.

4.1.2 Thermal behavior and catalyst percentage

As previously discussed, sodium chlorate contains less oxygen than lithium perchlorate and is only competitive when catalysts are used to reduce the decomposition temperature. Before developing a system that utilizes sodium chlorate to generate oxygen, a required step was to reproduce and expand upon the relevant literature. Figure 4-2 below shows the effects of varying percentages of microscale and nanoscale cobalt oxide catalysts on sodium chlorate. The weight loss profile for 0% cobalt oxide (pure sodium chlorate) approximated what was found in the literature [2], with the 50% DT occurring at 575°C, slightly higher than the 50% DT of approximately 560°C reported by Shafirovich [2]. Additionally, Figure 4-2 confirms that both microscale and nanoscale cobalt oxide are strong catalysts for the thermal decomposition of

sodium chlorate and that at catalyst weight percentages above 3%, nanoscale cobalt oxide has a greater effect than microscale cobalt oxide. This improved catalytic effect is most likely due to the greater surface area per mass associated with nanoparticles [31]. As described in Chapter 3, tests were conducted in nitrogen gas with a 10 ml/min flow rate through the balance chamber and a 25 ml/min flow rate through the furnace and that samples, weighing 10±2 mg, were heated at 20°C/min in a high-temperature platinum pan.

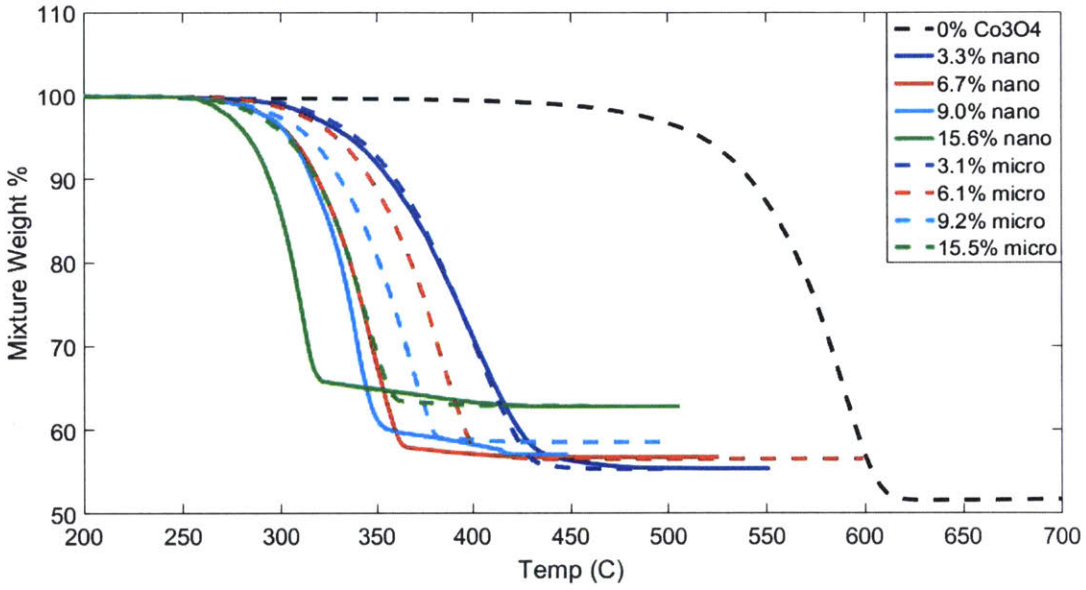

Figure 4-2: Results confirmed that decreased catalyst particle sizes and increased catalyst weight percentages resulted in lower decomposition temperatures.

Analysis showed the inclusion of 3.3% by weight nanoscale cobalt oxide reduced the 50% DT from 575°C (for pure sodium chlorate) to 387°C, much higher than the 50% DT of approximately 250°C achieved in the literature with only 3% nanoparticle cobalt oxide (see Figure 2-15). Further analysis (to be discussed later) was conducted to investigate differences between the results presented in this work and the literature, however for this project sodium chlorate mixtures with 6.7% by weight nanoscale cobalt oxide were used. Table 4.1 below summarizes the results from Figure 4.1.

Mixture	Wt. % Co_3O_4	50% DT (°C)	Wt. loss (%)	
			Measured	Theoretical
$NaClO_3$	0.0	574	48.3	45.1
$NaClO_3/Co_3O_4$ (micro)	3.1	388	44.7	43.7
$NaClO_3/Co_3O_4$ (micro)	6.1	370	43.5	42.3
$NaClO_3/Co_3O_4$ (micro)	9.2	352	41.4	40.9
$NaClO_3/Co_3O_4$ (micro)	15.5	334	37.1	38.1
$NaClO_3/Co_3O_4$ (nano)	3.3	387	44.6	43.6
$NaClO_3/Co_3O_4$ (nano)	6.7	338	43.2	42.1
$NaClO_3/Co_3O_4$ (nano)	9.0	333	42.9	41.0
$NaClO_3/Co_3O_4$ (nano)	15.6	305	37.2	38.1

Table 4.1: Theoretical weight losses were calculated from the stoichiometric oxygen available for decomposition. Differences between theoretical and measured weight loss percentages were most likely due to solid particles being ejected from the TGA pan and removed by the flue gas during testing. The existence of minor side reactions, such as those resulting in the production of chlorine gas, may also have contributed to these differences.

4.1.3 Identification of system operating temperature

In order to design an oxygen generation system, the first step was to choose a system operating temperature, as this would control the needed power requirements and have a strong effect on the rate of sodium chlorate decomposition and oxygen production. Figure 4-3 below shows the decomposition profiles for sodium chlorate and nanoscale cobalt oxide powder mixtures and the rate of mass loss during these experiments as a function of temperature. The results from these experiments are also functions of time, as the samples were being heated with a constant temperature increase of 20°C/min. The maximum rates of mass loss, occurring at the peaks found in the rights hand side of the figure, correspond to the inflection points found in the left hand side of the figure. Figure 4-3 indicates that the 6.7 wt.% cobalt oxide mixture achieved a maximum rate of mass loss of 20 wt.%/min at 344°C. However, this is not an accurate estimate as rates of decomposition typically depend on the concentration/amount of reactant that is available for decomposition. During these experiments, the gradual increase in temperature meant that the mixtures were

subject to several minutes of slow and moderate rates of decomposition. In an actual system, the heating would occur much faster, meaning much of the sodium chlorate would be unreacted by the time elevated temperatures have been achieved.

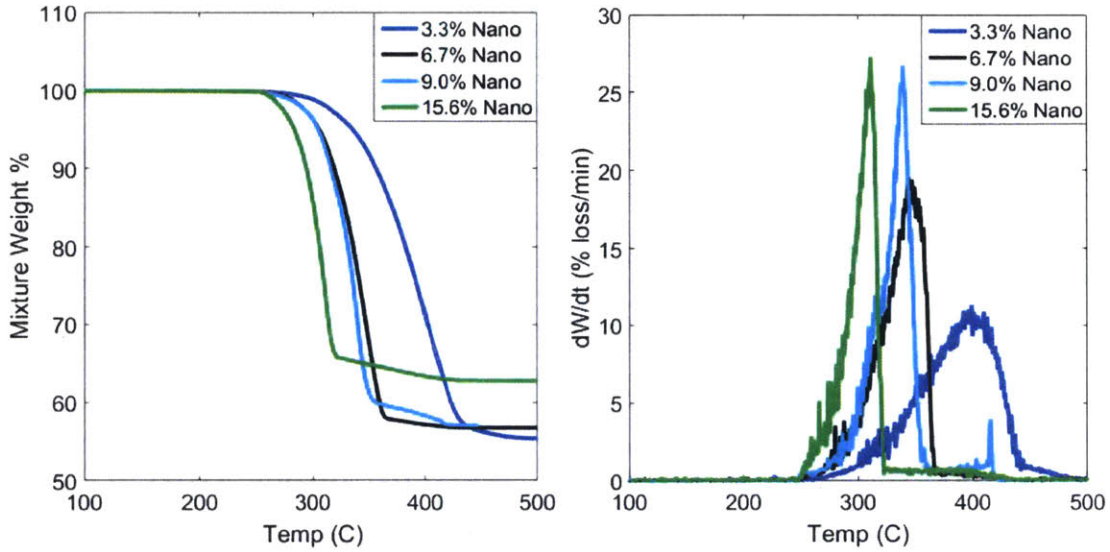

Figure 4-3: Significant portions of the samples decomposed before elevated temperatures were achieved, thus preventing potentially higher rates of decomposition from being observed.

To better understand the effect of temperature on the decomposition rate of catalyzed sodium chlorate, isothermal TGA tests were conducted, with the results being shown below in Figure 4-4. Samples containing 6.7 wt.% cobalt oxide were heated at 100°C/min, until the target temperatures of 300°C, 325°C and 350°C were reached. The samples were then held at these target temperatures until decomposition was complete, with the 350°C test being conducted twice to confirm the results. During each test, the 100°C/min temperature ramp began after the samples had been heated to an initial temperature of 50°C. Finally, the dashed lines seen in Figure 4-4 indicate the time at which each test had reached its target temperature and was designated as being isothermal.

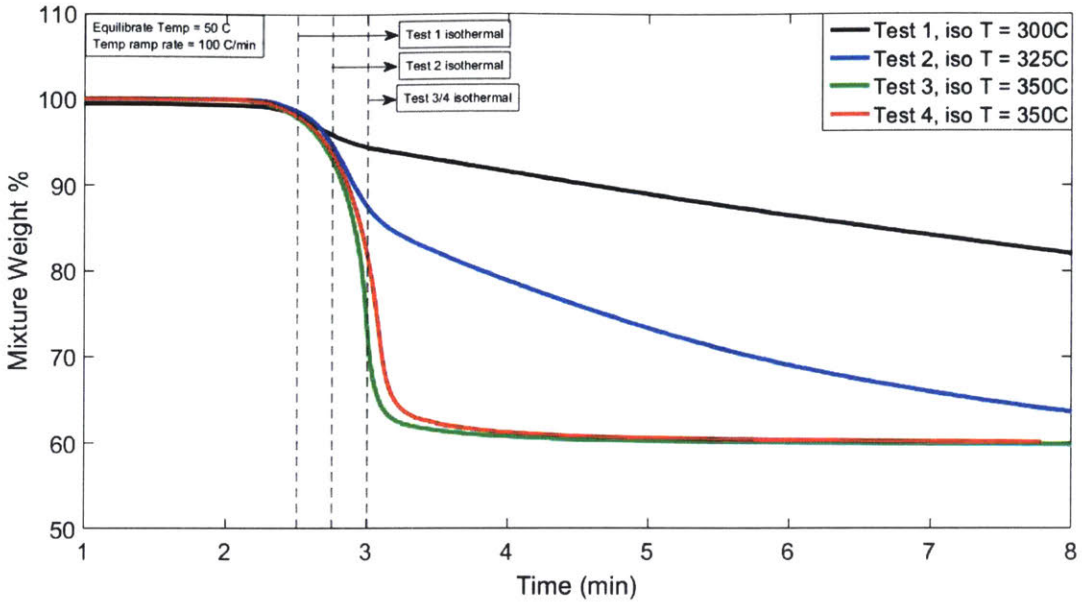

Figure 4-4: These results showed that, for a sodium chlorate mixture containing 6.7% by weight nanoscale cobalt oxide, 350°C is a suitable operating temperature.

When held at 300°C during test 1, the mixture decomposed slowly. This test was ended after 15 minutes of heating due to time constraints. When held at 325°C during test 2, the same mixture had a moderate rate of decomposition, with complete decomposition achieved after about 10 minutes. Finally, the same mixture decomposed rapidly when held at 350°C during tests 3 and 4. Because of how quickly the sodium chlorate was decomposing during test 3, the target isothermal temperature of 350°C was only achieved after the sample had lost 26% of its mass. Similarly, during test 4 the sample had lost 18% of its mass before reaching 350°C. These were significant losses in weight, as full theoretical decomposition for a sodium chlorate mixture containing 6.7 wt.% cobalt oxide would corresponds to a 42% loss in weight. Below, Figure 4-5 shows that tests 3 and 4 had maximum rates of mass loss of 205 wt.%/min and 134 wt.%/min, respectively. These decomposition rates were much faster than the observed maximum decomposition rate of 20 wt.%/min seen for the same mixture in Figure 4-3. Again, this higher rate was observed because the elevated temperature was reached at an earlier period in the decomposition process.

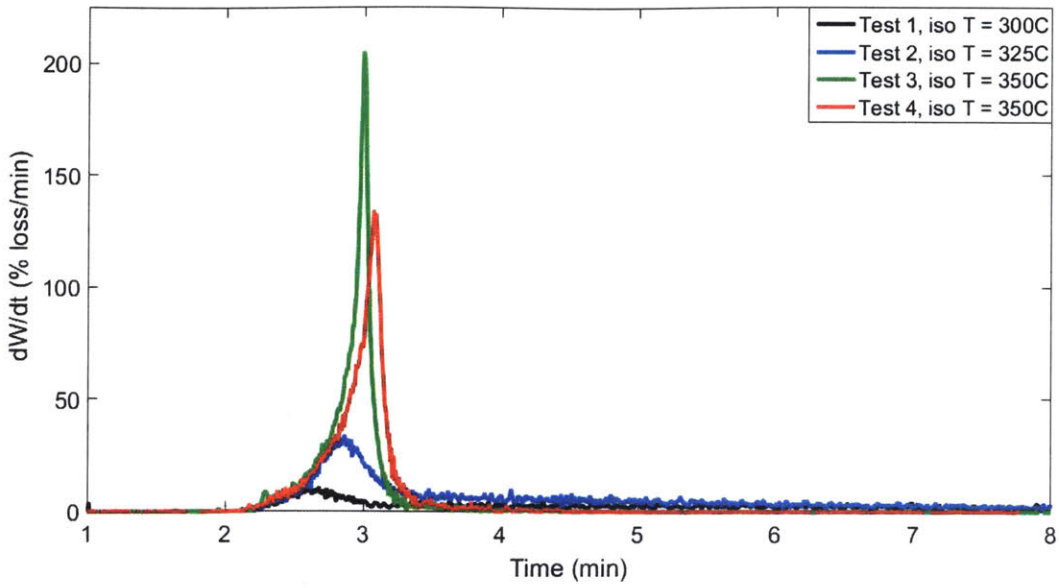

Figure 4-5: Though not performed, it is suspected that using temperature ramp rates greater than 100°C/min would have resulted in the observation of even faster rates of decomposition.

The above results indicate that 350°C is an ideal operating temperature for a sodium chlorate mixture containing 6.7 wt.% cobalt oxide. Because of how quickly decomposition proceeds, the rate of oxygen production for a system using this mixture and operating temperature would be controlled by how quickly the reactants can be heated to 350°C, but not how long the reactants are held at this temperature.

4.1.4 Chlorine gas and the effects of lithium peroxide

When selecting sodium chlorate as an oxygen storage medium, another consideration is the purity of the produced oxygen. As shown in Equation 2.5, one possible side reaction results in chlorine gas, which is both toxic and corrosive. Chlorine removal is critical in breathing applications, however its removal may also be important in power systems due to added complications with system design and material compatibility. For example, dry chlorine (elemental chlorine with very low water content) is compatible with 316 series stainless steels, but should not be used with plain carbon steels, aluminum, brass and titanium [36]. Furthermore, when in the presence of

trace amounts of water, chlorine gas forms corrosive compounds and is incompatible with most metals [37]. Two of the most common chlorine scavengers are barium peroxide and lithium peroxide. These compounds, which adsorb the chlorine, are also known to be mild catalysts for the decomposition of sodium chlorate [30]. Figure 4-6 shows the effect of lithium peroxide on the decomposition of sodium chlorate. Initial mass losses exhibited during these tests, which generally occurred between 300°C and 400°C, were due to the lithium peroxide decomposing into oxygen and lithium oxide (Li_2O). This likely means that lithium oxide is the catalyst for the decomposition of sodium chlorate and not lithium peroxide. The results largely agree with the work done by Cannon and Zhang [30], with lithium peroxide weight percentages above 2% having little to no additional catalytic effect on the sodium chlorate decomposition temperature. Based on the 50% DT, all lithium peroxide mixtures decomposed rapidly between 498°C and 532°C. These results are also summarized in Table 4.2.

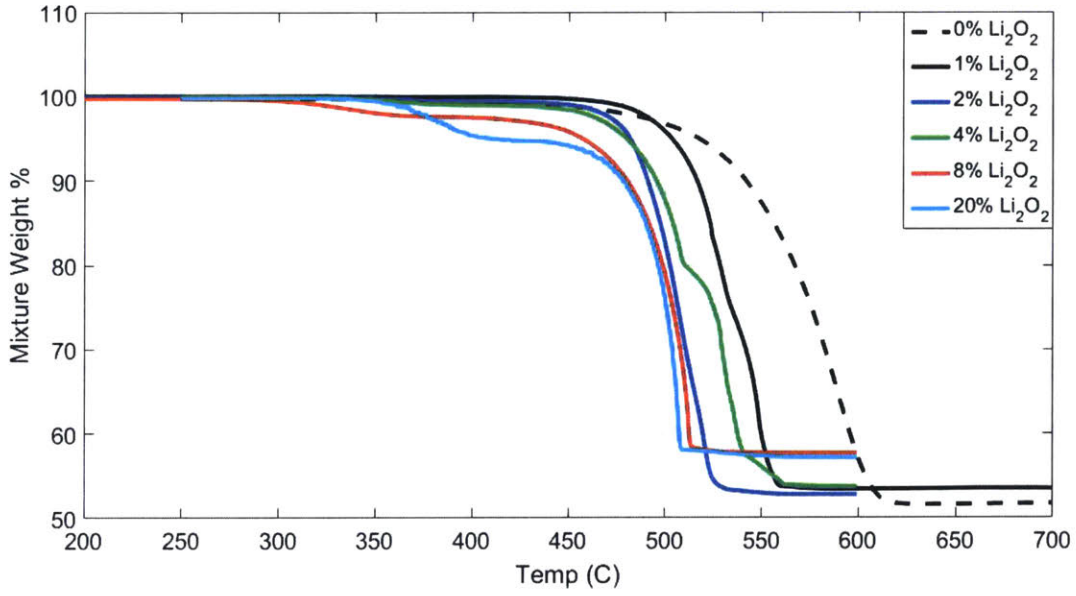

Figure 4-6: Though useful as a chlorine suppressant, lithium peroxide does not substantially reduce sodium chlorate's decomposition temperatures.

Mixture	Wt. % Li_2O_2	50% DT (°C)	Wt. loss (%)	
			Measured	Theoretical
$NaClO_3$	0	574	48.3	45.1
$NaClO_3/Li_2O_2$	1	532	46.5	45.0
$NaClO_3/Li_2O_2$	2	506	47.3	44.9
$NaClO_3/Li_2O_2$	4	522	46.3	44.7
$NaClO_3/Li_2O_2$	8	500	42.4	44.3
$NaClO_3/Li_2O_2$	20	498	42.9	43.1

Table 4.2: As shown in the literature, small weight percentages of lithium peroxide reduced the 50% DT to around 500°C, with larger percentages of lithium peroxide having negligible effects.

As lithium peroxide is primarily used for its chlorine scavenging properties, and not its mild catalytic effects, additional catalysts and/or metal fuels are typically added to lithium peroxide and sodium chlorate mixtures. Previous work has shown that lithium peroxide partially suppresses the catalytic effect of cobalt oxide, with rapid decomposition for mixtures containing between 1% and 8% by weight lithium peroxide occurring between 380°C and 417°C. Figure 4-7 and Table 4.3 below shows the decomposition profiles for several triple mixtures of lithium peroxide, nanoscale cobalt oxide and sodium chlorate. These results indicate that lithium peroxide has an even stronger inhibiting effect on the cobalt oxide catalysis of sodium chlorate, as rapid decomposition (based on the 50% DT) only occurred between 496°C and 500°C. This inhibiting effect of lithium peroxide is significant as it does not allow sodium chlorate to be competitive with lithium perchlorate as an oxygen source. Shown above in Figure 4-1, sodium chlorate requires significantly more power to extract the same amount oxygen than lithium perchlorate when temperatures needed for rapid decomposition exceed 350°C. As such, future sodium chlorate oxygen systems with limited power budgets should rely on chlorine removal processes that occur after and not during the production of oxygen.

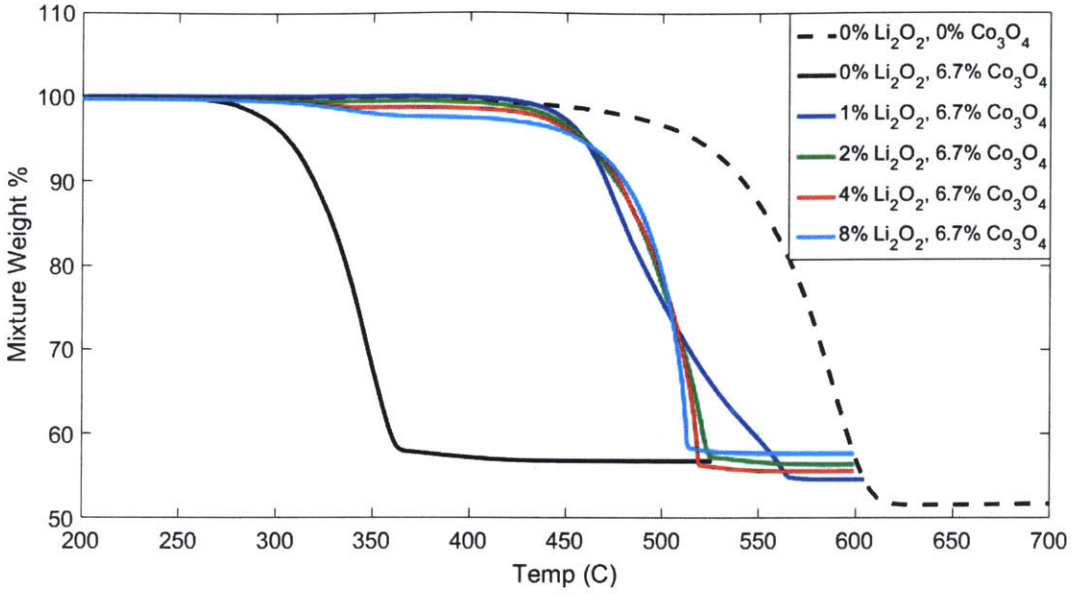

Figure 4-7: The inclusion of only small amounts of lithium peroxide suppresses the catalytic effect of cobalt oxide. Increased amounts of lithium peroxide seemed to have no additional effects.

Mixture	Composition (Wt. %)		50% DT (°C)	Wt. loss (%)	
	Co_3O_4	Li_2O_2		Measure	Theoretical
$NaClO_3$	0	0	574	48.3	45.1
$NaClO3/Co_3O_4$	6.7	0	338	43.2	42.1
$NaClO_3/Co_3O_4/Li_2O_2$	6.7	1	496	45.5	42.0
$NaClO_3/Co_3O_4/Li_2O_2$	6.7	2	499	43.7	41.9
$NaClO_3/Co_3O_4/Li_2O_2$	6.7	4	501	44.5	41.7
$NaClO_3/Co_3O_4/Li_2O_2$	6.7	8	500	42.4	41.3

Table 4.3: This table summarizes the chemical compositions and testing results from Figure 4-7.

Thermogravimetric analysis with attached mass spectrometry (TGA-MS) was used to analyze the decomposition products from pure sodium chlorate and from mixtures containing cobalt oxide. The goal was to observe chlorine production and then perform the same analysis with mixtures containing the chlorine-scavenging lithium peroxide. However, chlorine gas was not detected during the baseline tests, resulting in the lithium peroxide mixtures not being subject to the same analysis. The lack of chlorine detection may have been due to user error or equipment sensitivity. Another

explanation is that chlorine contamination is only a problem when sodium chlorate is used in oxygen candle formulations. Water leftover from the manufacturing process and the type of incorporated binder can promote the formation of hypochlorous acid, chlorine gas and chlorine dioxide [38]. Furthermore, chlorine impurities are associated with the high internal temperatures present in oxygen candles [31, 38].

4.2 Disagreement with literature results

Cobalt oxide is an excellent catalyst for the decomposition of sodium chlorate, with literature results showing that rapid decomposition can be achieved with temperatures as low as 245°C. However, during this project, rapid decomposition with catalyst weight percentages similar to those found in the literature required temperatures between approximately 93°C and 137°C greater than was expected. As shown in Figure 4-1, a sodium chlorate system requiring a 350°C decomposition temperature versus a 250°C decomposition temperature would require at least 50% more power to produce the same amount of oxygen. Because of this discrepancy, additional tests were conducted to determine if the differences between the literature and presented results were due to catalyst surface areas, mixture preparation techniques or artifacts of the testing conditions.

4.2.1 Effect of cobalt oxide catalyst surface area

Table 4.4 summarizes the TGA results from various authors who studied the decomposition of sodium chlorate catalyzed with cobalt oxide and compares the results to those found during this project. It shows that cobalt oxide catalysts characterized by smaller length scales and larger specific surface areas (m^2/g) provide greater catalytic effect. The nanoscale cobalt oxide used during this project was advertised as having a surface area between 40 m^2/g and 70 m^2/g, which is why results similar

to those found by Wydeven, whose catalyst had a surface area of 67 m^2/g, were expected. Furthermore, the microscale and nanoscale catalysts used during this project were purchased from the same supplier and were advertised as having the same characteristic particle sizes as the catalysts used by Shafirovich, also indicating similar results should have been obtained.

Lit. Source	Wt. % Co_3O_4	50% DT (°C)	Catalyst BET Surface Area (m^2/g)	Catalyst Particle Size (μm)
Wydeven	6.8	245	67	0.015
	18.4	325	0.75	1.3
Zhang	1	273	150	NA
	8.4	255	61	NA
	8.4	350	5	NA
Shafirovich	3	250	NA	0.05
	3	350	NA	10
J. Garcia	3.3	387	40-70	0.05
	6.7	338	40-70	0.05
	15.6	305	40-70	0.05
	3.1	388	NA	10

Table 4.4: Small particles have higher specific surface areas and are often more active catalysts.

Surface area analysis conducted by this author indicated that the nanoscale and microscale cobalt oxide had specific surface areas of 1.16 m^2/g and 0.71 m^2/g, respectively. The surface area of the nanoscale catalyst was significantly less than what was advertised and is likely why high temperatures were required for decomposition. Figure 4-8 shows a sodium chlorate mixture containing 6.7% by weight nanoscale cobalt oxide that had been ground with a mortar and pestle. The smooth particles occupying most of the image are sodium chlorate, while the particles with a cauliflower-like appearance are cobalt oxide. It was not confirmed if the masses of cobalt oxide were individual particles or agglomerates of many particles.

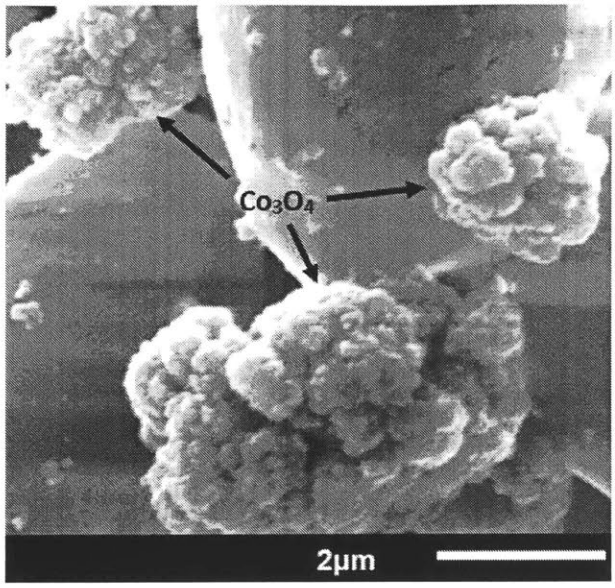

Figure 4-8: Agglomeration of the catalyst could explain the different surface areas advertised by the supplier and measured by this author. The agglomerates acted as larger particles with smaller specific surface areas would.

4.2.2 Effects of TGA procedures and mixture preparation

Other possible reasons for variations between this work and the literature include differences in TGA testing procedures and non-uniformity of the prepared mixtures. Variables that can affect the reproducibility of TGA results include the calibration and cleanliness of the equipment, the size of the sample that is to be tested, the type and flow rate of the gas used in the equipment and the temperature scanning/ramp rate used to heat the sample. Table 4.5 gives the TGA conditions used to produce the results that are shown above in Table 4.4. After reducing the heating rate from 20°C/min to 10°C/min, the 50% DT for for mixtures containing the microscale catalysts agreed to within 3% of the results presented by Shafirovich. However, both reducing the heating rate and increasing the furnace flow rate to match the conditions used by Shafirovich did not bring the nanoscale catalyst results into agreement with the literature.

Lit. Source	TGA Testing Conditions				
	Heating Rate (°C/min)	Purge Gas	Furnace Flow Rate (ml/min)	Balance Flow Rate (ml/min)	Sample Size (mg)
Wydeven	10	N_2	30	NA	3.94
Zhang	20	O_2	150	NA	100
Shafirovich	10	Ar	90	10	10
J. Garcia	20	N_2	25	10	10

Table 4.5: Though useful, TGA results are affected by the various testing conditions. The rate at which samples are heated typically has the largest effect, although even the orientation/arrangement of a sample in the testing pan can impact the results.

Scanning electron microscopy, shown below in Figure 4-9, was used to compare the nanoscale cobalt oxide and sodium chlorate mixtures prepared by this author to those found in the literature. See Appendix C for additional SEM images taken during this project. Below, images A and B show mixtures containing 3% by weight nanoscale cobalt oxide and were prepared by Shafirovich and A. Garcia [2, 39]. Their results showed that there was no significant difference between the decomposition of samples that had been mixed using a ball mill at 1100 rpm (image A) and samples that had been mixed by hand using an agate mortar and pestle (image B). Because about two thirds of the sodium chlorate decomposed in the liquid state, they posited that capillary spreading lessened the importance of sodium chlorate particle size and powder uniformity [2]. Images C and D show samples containing 6.7% by weight nanoscale cobalt oxide and were prepared by this author. The image C sample, which is less uniform than the literature samples and characterized by larger sodium chlorate particle sizes, was ground for 5 minutes using a porcelain mortar and pestle. Lastly, the sample shown in image D was stirred for 5 minutes using a glass stirring rod and in a glass beaker. This sample was prepared rather crudely so as to further assess the effects of sodium chlorate particle size.

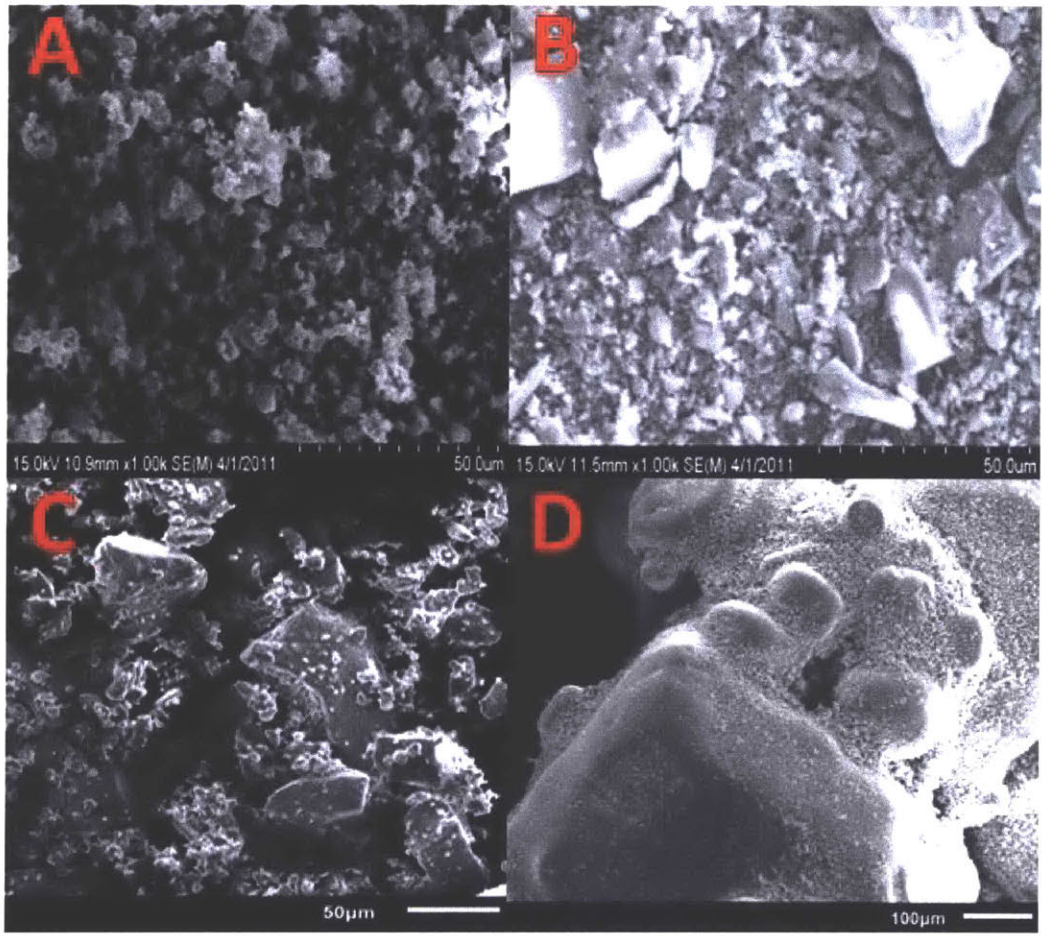

Figure 4-9: Samples A and B, containing 3% by weight cobalt oxide, were found in the literature, while samples C and D, containing 6.7% cobalt oxide, were prepared by this author. Samples B and C were prepared using similar procedures.

Figure 4-10 below shows the TGA decomposition profiles for several mixtures containing 6.7% by weight nanoscale cobalt oxide. Altering the furnace flow rate and sodium chlorate particle size (see images C and D in Figure 4-9) had little to no effect on the decomposition profiles. Slowing the heating rate to 10°C/min slightly reduced the 50% DT to 328°C, however this was still much higher than the 250°C reported by Shafirovich and shown in Table 4.4 (using the same heating rate, sample size, catalyst size and smaller catalyst percentage).

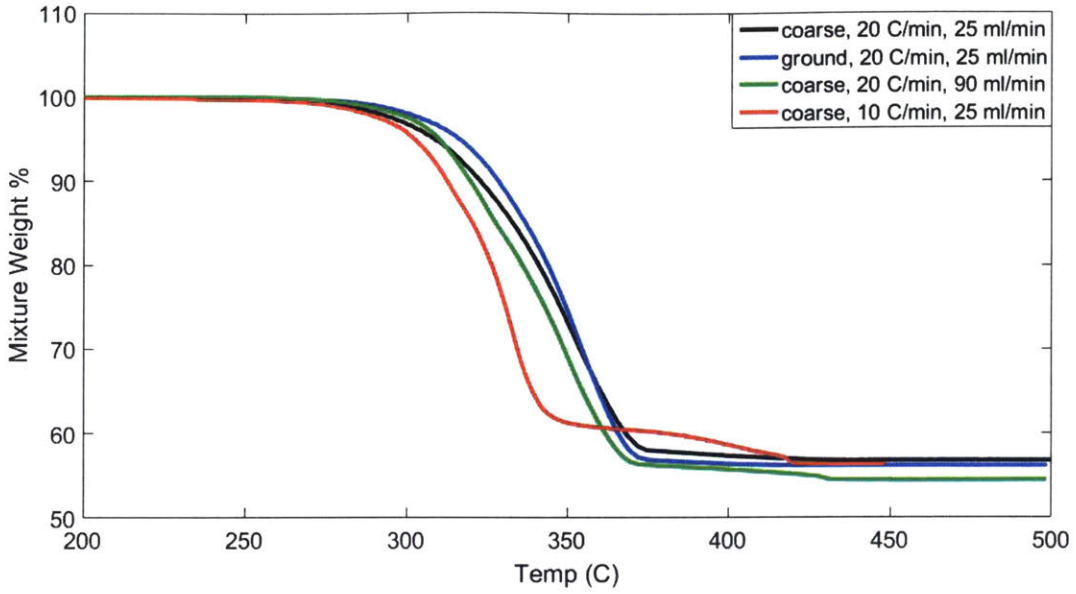

Figure 4-10: Different TGA testing procedures and sample mixing techniques played only a minor role in the discrepancy between these results and those in the literature. The differences were likely due to inadequate preparation/storage of the nanoscale catalyst, either by this author or the supplier.

Differences between the results in this work and the literature were likely due to the use of a catalyst with a smaller surface area and variations in both testing procedures and mixture preparation. Though left as future work, addressing these issues is critical to making sodium chlorate competitive with other oxygen storage methods. Achieving rapid decomposition at temperatures around 250°C will allow for significantly reduced power requirements. Additionally, doing so with low catalyst weight percentages ($\leq$3%) will further improve the gravimetric and volumetric energy densities of a potential system while making sodium chlorate more competitive from a cost standpoint, as cobalt oxide, based on Sigma Aldrich prices, is 25 to 40 times as expensive as sodium chlorate [32]. Finally, cobalt oxide is carcinogenic and toxic, making the use of this material in smaller weight percentages desirable.

THIS PAGE INTENTIONALLY LEFT BLANK

Chapter 5

Prototype Development

This section discusses the development and testing of two methods for oxygen generation using sodium chlorate. The first concept relied on using a 304 stainless steel bead chain to drag the sodium chlorate mixture into a heated tube where it would be heated until decomposition. Operated on a continuous basis, the chain would simultaneously remove reacted wasted products from the chamber. Work on this concept focused on reproducing results from previous students at MIT and identifying its key problems. The second concept relied on a batch process that involved the loading of several grams of sodium chlorate mixture into a 316 stainless steel reaction chamber, the heating of the mixture until decomposition via heaters external to the reaction chamber and the subsequent ejection of the waste products with a piston. Pure sodium chlorate and mixtures with 6.7% nanoscale cobalt oxide were used during the testing of these systems. As discussed in the previous chapter, TGA results indicated no difference in the thermal decomposition between mixtures that had been prepared with a glass stirring rod and beaker and those that had been prepared with the mortar and pestle. Because using the glass stirring rod and beaker simplified laboratory clean up and allowed for larger amounts of mixtures to be prepared at one time, this method was used to prepare mixtures during this portion of the project.

5.1 Bead Chain System

5.1.1 Initial Chemical Testing

Previously this author only reacted relatively small amounts of sodium chlorate and cobalt oxide mixtures ($\leq$1 gram). To gain a better understanding of how to work with and handle the chemicals, progressively larger amounts were heated to decomposition with a laboratory hot plate. Figure 5-1 shows the decomposition of 20 grams of sodium chlorate with cobalt oxide. Bubbles due to the release of oxygen gas were observed before the material had fully liquefied. Bubble formation gradually increased until the 7:44 min mark, at which point there was a violent release of oxygen and heat, quickly bringing the reaction to completion.

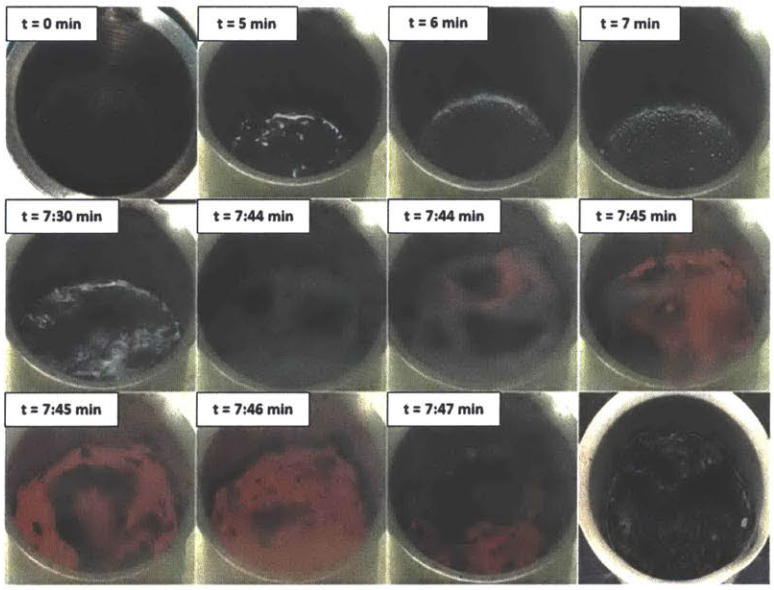

Figure 5-1: The samples were contained in a 316 stainless steel beaker and the hot plate was maintained at approximately 500°C. Transitioning from being a solid to a liquid and finally back to being a solid complicates the transport of sodium chlorate mixtures into and out of a reaction chamber. The exothermic release of heat during decomposition also has the potential to prematurely melt portions of the mixture or possibly damage the system due to spikes in temperature.

5.1.2 Unheated Drag Tests

The first step in assessing the feasibility of a bead chain system was to determine if the chain could adequately transport unheated sodium chlorate mixtures. A powder hopper was attached to the end of 316 stainless steel tube which had an inner diameter of 0.194 in. A 304 stainless steel bead chain with a bead diameter of 0.1875 in was threaded through the stainless steel tube. Figure 5-2 illustrates this basic setup:

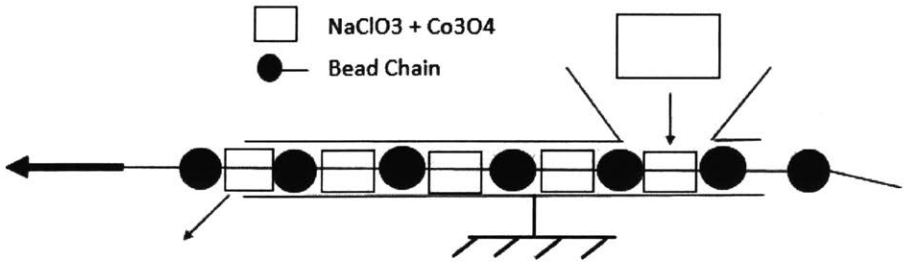

Figure 5-2: The tubing and hopper assembly was supported with a typical laboratory stand. The ball chain was threaded through the tubing and connected end-to-end.

After loading the hopper with 10 grams of sodium chlorate, the chain was slowly ($\approx$0.5 cm/s) dragged by hand through the tubing. The majority of the powder readily flowed through the tubing, with the exception of a few clumps that were equal or greater in size than the tube diameter. This test was repeated with a sodium chlorate and cobalt oxide mixture with no added difficulty.

5.1.3 Heated Drag Tests

Next, a 50 W heat cable was attached to the end of the tubing and wrapped in mineral wool insulation. Figure 5-3 offers a schematic of the setup, which had the heat cable and insulation covering 6 inches of the 12 inch tubing. The steel tubing was allowed to heat up for ten minutes after which thermocouple measurements along the inside of the tubing indicated temperatures equal to or exceeding 450°C. Afterwards, 10 grams of sodium chlorate were loaded into the hopper and the chain was

again slowly pulled by hand through the tubing. Within 15-20 seconds, the chain seized inside the tubing and could not be removed by hand. Because this mixture was uncatalyzed and the system temperatures were not high enough to decompose sodium chlorate, the cause of the jam was most likely due to uneven transport of molten sodium chlorate. Upon entering its liquid state, capillary spreading resulted in the molten sodium chlorate mixing with unmelted sodium chlorate that had not yet entered the heated regions of the tubing. This liquid/solid mixture quickly became impossible to transport, as its temperature fell below 250°C and turned into a frozen mass. The same result was observed after loading the powder hopper with the catalyzed mixture. After increasing the size of the tubing so that it had an ID of 0.44 inches, the chain no longer froze within the tubing. Waste products, attached to the chain, were observed exiting the tube after about 10 minutes of chain motion. Because the ratio of the tubing to chain diameters was more than doubled from ≈1 to 2.3, conveying the powder to the end of the tubing required significantly more time.

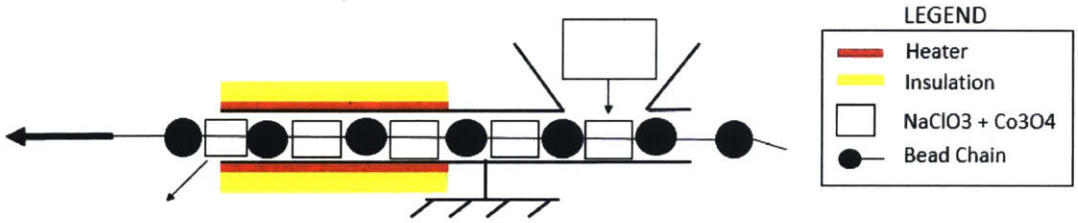

Figure 5-3: As with the previous experiment, this assembly was mounted in the fume hood with a laboratory stand.

5.1.4 Prototype Results

To further investigate if the bead chain was an effective method for conveying sodium chlorate mixtures through a heated reaction chamber, the previous experiments were repeated with a servo being used to pull the chain and powder mixtures. This allowed for accurate control over the speed of the chain, for longer tests to be conducted and was closer to an actual oxygen system. Figure 5-4 offers a schematic

of the system and Figure 5-5 shows the experimental setup. Though basic in its design, this modular setup allowed for each of the chain, tubing, heat cable, servo and sprocket to be quickly changed out if need be. Additionally, pulleys and supports were easily adjustable, ensuring tension in the chain.

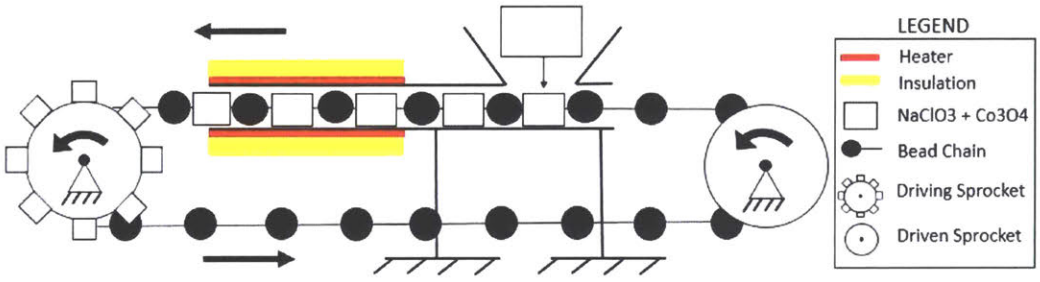

Figure 5-4: Experimental schematic of the final bead chain prototype.

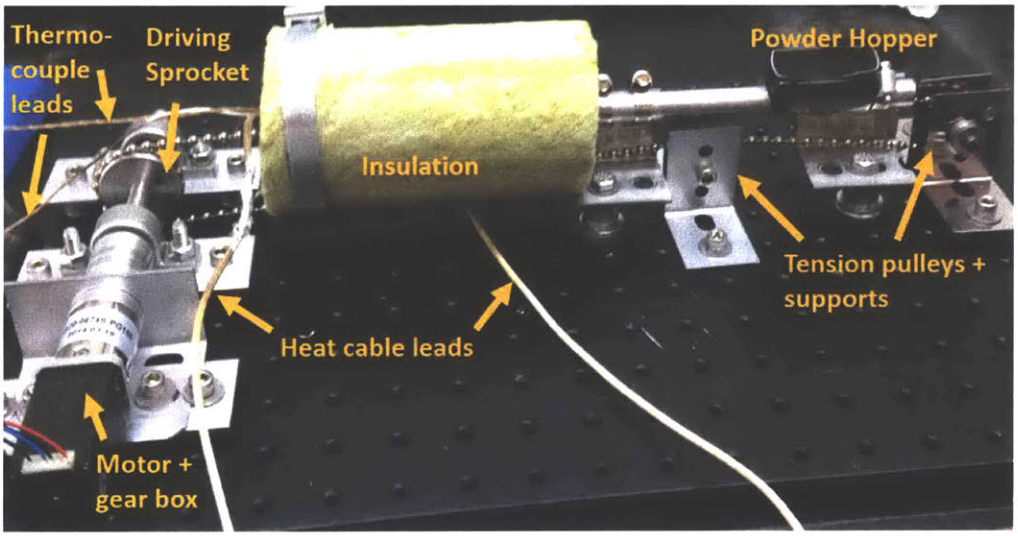

Figure 5-5: Though simple in design, this system struggled to transport the fully liquid material and was prone to jamming. Utilizing a more active cobalt oxide catalyst may improve results, as some of the mixture would decompose prior to reaching the melting point and thus not enter a liquid state.

As was experienced during previous experiments, the bead chain quickly jammed inside the heated tubing when their diameters were approximately equal. Using a tubing with an inner diameter of 0.44 inches (with chain diameter of 0.1875 inches) once again prevented the system from immediately jamming. Several tests were conducted, with the lengths of the tests varying between one to two hours. Instead of

being effectively conveyed through the tubing, the solid and molten mixtures slowly built up along the inside of the tubing and near the entrance and exit of the heated area. The solidified buildup at the entrance of the heated region was composed primarily of unreacted sodium chlorate and catalyst, while the buildup at the exit of the system was a partially decomposed mixture containing, sodium chlorate, sodium chloride and the cobalt oxide catalyst. Because of this, each test ended when the inner diameter of the tubing had been reduced enough to jam and eventually snap the chain, which had a yield strength of 40 lbs. Another issue during these longer tests was corrosion of the 304 stainless steel bead chain, resulting in the reddish and black/green products shown below in Figure 5-6.

Figure 5-6: The 304 stainless steel chain suffered from corrosion during longer tests. Sodium chlorate melt also tended to fill the hollow beads during transport through the reaction chamber, reducing flexibility of the chain.

Implementing a bead chain sodium chlorate oxygen system was left as future work. The work of previous students, who met with more promising results, was not successfully reproduced. Better design and improved insulation would likely improve the reliability of this type of system while reducing heat losses, however the issues faced by this system were similar to the issues encountered by systems in the literature. For example, both of the lithium perchlorate oxygen systems discussed in Sections 2.3.1 and 2.3.2 were subject to failures caused by the solidification of both unreacted

and reacted chemicals at the entrances and exits of their systems. Due to the relatively high melting points of sodium chlorate and lithium perchlorate, systems that rely on pumps or mechanical methods to transfer these chemicals in their molten states run the risk of failure if the chemicals resolidify/freeze. Furthermore, the high melting points of their respective waste products, sodium chloride and lithium chloride, complicate the waste removal process as they are even more likely to freeze and accumulate inside a system's reaction chamber.

5.2 Batch Piston System

5.2.1 Overview

This section discusses the development of a batch process for the decomposition of sodium chlorate. The unheated chemicals were loaded by hand into the reaction chamber, heated until decomposition, ejected and then removed by hand. Figure 5-7 shows these basic steps:

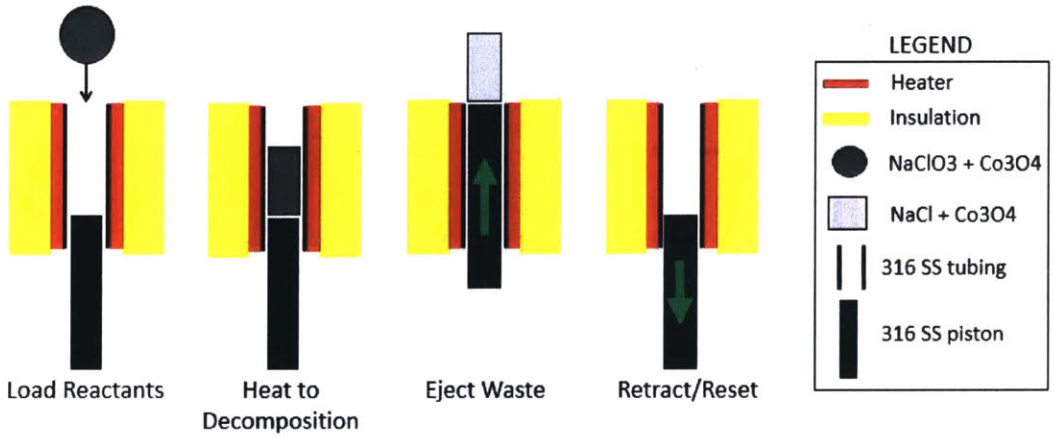

Figure 5-7: Despite the open construction of the reaction chamber, it was expected that only a small percentage of sodium chlorate would leak from the system. Due to its high melting point, any sodium chlorate leaking from the reaction chamber quickly freezes, preventing further loss of material.

5.2.2 Initial Tests

To size the servo used to operate the piston, an estimate of the force required to eject the waste materials was needed. A 316 stainless steel piston and tubing were machined and then mounted with a laboratory stand, shown below in Figure 5-8. Hose clamps secured the heat cable to the portion of the tubing serving as the reaction chamber. The tubing was approximately 3 inches long with an inner diameter of 0.439 inches. A tapered reamer was used to apply a one degree internal taper along 2 inches of the tubing, increasing the inner diameter at one end of the tubing to 0.479 inches. The addition of this taper meant that the piston would be unable to clear the entire volume of the reaction chamber, but also served to reduce the force required for waste ejection. The piston head had a diameter of 0.428 inches and length of 0.75 inches. A power controller was used to limit the output of the heat cable to 25 W, with thermocouple measurements indicating that reaction chamber wall temperatures were equal to or greater than 350°C and that the surface of the piston was approximately 250°C. Two grams of catalyzed sodium chlorate was loaded into the reaction chamber and allowed to sit for 15 minutes, after which the heat cable and insulation were removed and the materials allowed cooled to room temperature.

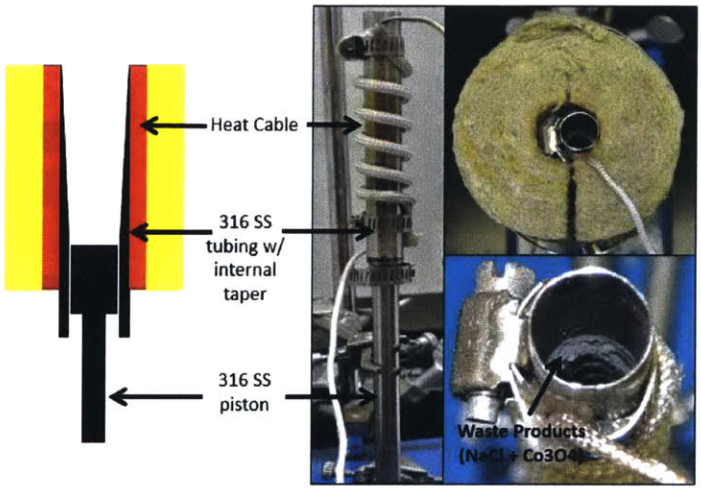

Figure 5-8: To avoid material corrosion issues, the piston and tubing were made from 316 stainless steel. This proved effective, as undesired species were not observed in the waste materials.

The tubing, piston and waste materials were later mounted in an Admet universal testing machine, which required 7 lbf to remove the waste when operated with a 5 mm/min advance rate. This was repeated after reducing the clearance between the piston head and tubing inner diameter from 0.011 inches to 0.006 inches, with similar results being obtained. As such, a linear servo with a maximum dynamic thrust of 25 lbf and a 6 inch stroke length was obtained for operating the piston. In order to assess whether or not the reaction had been carried to completion, waste products were collected and subject to additional heating. Based on the mixture stoichiometry, the results showed that 98% of the available oxygen had been released. There was concern that liquid sodium chlorate would leak into the gap between the piston and tubing and remain unreacted, however the high reaction completion and corresponding oxygen yield showed that this was at most a minor issue.

5.2.3 Prototype Results

To further assess this method of sodium chlorate decomposition, a servo was added to the same experimental setup. This allowed for the manual loading, decomposition, waste ejection and manual waste collection steps to be carried out continuously. Tests varied between approximately 20 minutes and 1.5 hours, with each cycle requiring 3 minutes to 3.5 minutes to heat 2 grams of catalyzed sodium chlorate to decomposition. Shorter tests were generally terminated after the piston jammed inside the reaction chamber, however in each case this mode of failure was due to improper alignment between the piston and tubing. The longer tests were terminated due to the durability of the fiberglass heat cables, which would fail after 2-3 hours of use. The longest and most successful test, which lasted 99 minutes, produced oxygen gas at a rate of 0.28 g/min or 0.21 L/min at NTP. This rate of oxygen production was calculated using the mixture stoichiometry and 99% reaction completion (obtained from post-test waste product heating). Burn-out of the heat cables, which were rated for operation up to

480°C, was likely due to a combination of poor contact between the cable and the surface of the tubing, shifting of the cable during operation causing contact between its coils and possibly high local temperatures caused by exothermic heat release during sodium chlorate decomposition. Figure 5-9 below shows the experimental setup:

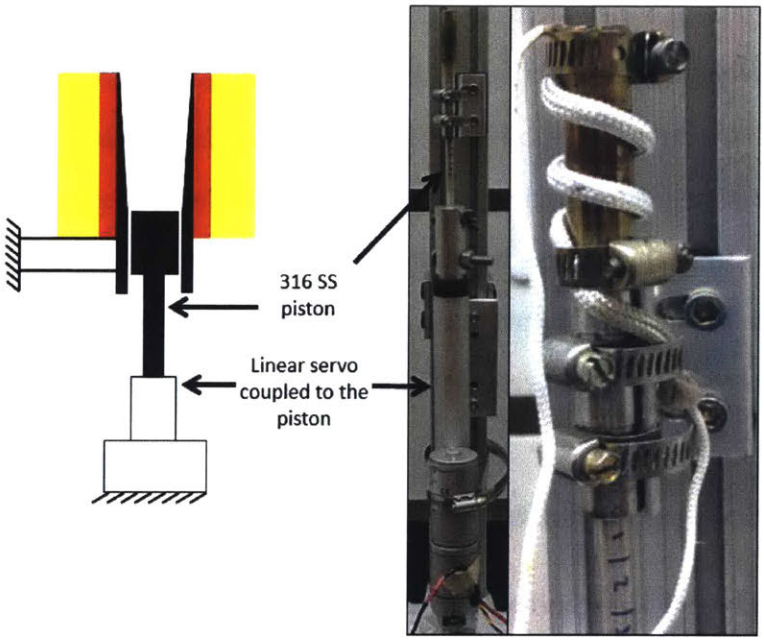

Figure 5-9: The discoloration of the stainless steel was due to high temperature growth of the oxidation layer and not chemical corrosion. The brown and purple colors on the outside of the tube, observed during this test and others, suggest that local temperatures were between 390°C least 450°C [40].

Figure 5-10 shows the system during various stages of operation. The left-most images are of the system during the decomposition step, with solidified waste products protruding from the reaction chamber exit and the mid-figure images are of the waste products after being ejected from the reaction chamber by the piston. The right-most images show the system after the waste had been removed by hand and the piston had been returned to its starting position. As is shown below, this was a messy process, with the internal taper of the reaction chamber resulting in some waste products not being removed during the ejection step.

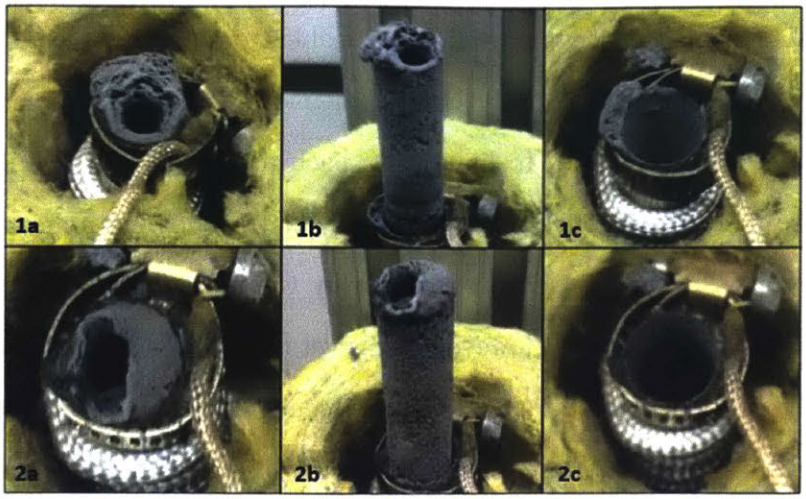

Figure 5-10: Using a piston to physically sweep the reaction chamber meant that failures due to the gradual buildup of frozen reactants and waste materials, the most common failure mode for these types of systems, is unlikely to occur.

Figure 5-11 shows what the waste products looked like after losing 99% of their available oxygen (left) and after losing only 85% of their available oxygen (right). In general, the partially decomposed products were packed more densely than those that were fully decomposed and tended to disintegrate more easily. The fully decomposed waste products formed into a hard but brittle cylindrical pellet.

Figure 5-11: Further refinement and more careful design of this batch process is needed. During one test, the piston head rested lower inside the reaction chamber than was intended. This reduced the temperature of the piston head and the adjacent reactants, resulting in incomplete decomposition (right).

Testing of this batch concept proved to be viable from a mechanical standpoint, as the system was able to effectively handle chemicals that, at different stages of operation, transition from solid, to liquid and back to solid states. While the previous bead chain conveyor concept had no difficulty transporting unheated sodium chlorate mixtures, the system struggled to convey the materials in their liquid and post-decomposition solid states. However, it has yet to be proven if this batch system is viable in terms of power requirements. Experiments testing the batch system were not optimized to reduce heat losses or increase the rate of sodium chlorate decomposition. Due to the geometry of the reaction chamber, no more than 2 grams of mixture could be decomposed per cycle. When greater amounts were loaded into the system, portions of the partially unreacted mixture would be ejected by the rapid release of oxygen gas. Furthermore, a cycle time less than 3 minutes was not achieved. This time was governed by how long it took to increase the temperature of the 2 grams of catalyzed sodium chlorate from room temperature, 20°C, to at least 350°C, the temperature at which rapid decomposition of this mixture was shown to occur. These limitations resulted in a maximum oxygen production rate of 0.21 L/min with a heating rate between 25 W and 33 W, well below the target 1.13 L/min (the oxygen flow required for a 200 W PEM fuel cell). The servo constantly drew approximately 1.5 W, although during the ejection step, which typically required 4 seconds of operation, the servo drew between 18 W and 30 W. Further assessment of this method requires a larger reaction chamber capable of reacting more sodium chlorate per cycle and better insulation to reduce heat losses and decrease cycle times. For example, the reaction chamber was bracketed directly to the 80-20 supports, which acted as a large heat sink. Adding some degree of thermal isolation to the reaction chamber would reduce these conductive losses and help maintain high reaction chamber temperatures. Finally, using a more active cobalt oxide catalyst would drastically improve the performance of this system. As was shown in Figure 4-1, reducing the

50% DT for catalyzed sodium chlorate from 350°C to 250°C would reduce the heating requirements by 35%. Future implementation of this method in a power system will require the use of an oxygen plenum. As this is a batch process, there are long periods of time with little to no oxygen release, followed by short periods of time characterized by rapid oxygen generation. An auxiliary gaseous oxygen tank would allow for the storage of excess oxygen while ensuring that the flow rate matches the variable demand of a fuel cell. It should be noted that the inclusion of intermediate gaseous storage for oxygen flow rate leveling would reduce the system's gravimetric and volumetric oxygen storage densities.

THIS PAGE INTENTIONALLY LEFT BLANK

Chapter 6

Summary and Conclusions

In this thesis we investigated the use of sodium chlorate as an oxygen storage medium for use in a fuel cell power system. When used in existing oxygen candles, sodium chlorate has already proven to have a greater volumetric oxygen density than existing liquid oxygen systems. Furthermore, oxygen candles provide both space and weight savings when compared to gaseous oxygen systems pressurized to 3000 psi. However, implementing sodium chlorate in a fuel cell power system will require fine control over the rate of chemical decomposition and corresponding oxygen release, a feature that is not offered by oxygen candles. Due to the high temperatures required for decomposition, oxygen candles contain metal fuels that, once ignited, release enough heat to ensure self-sustained combustion front propagation inside the candle assembly. This makes oxygen candles useful for emergency situations, but not in power systems.

During this project we developed a batch method for releasing oxygen from sodium chlorate. Mixtures catalyzed by cobalt oxide were loaded into a reaction chamber and heated until decomposition. Afterwards a piston was used to eject the materials from the reaction chamber. This method proved to be safer and more reliable than similar systems as the primary modes of failure, those associated with the buildup of solid residue at the inlets and exits of the reaction chamber, were removed. Aside from

preventing the flow of oxygen to a fuel cell, these modes of failure are dangerously unacceptable as they can lead to reaction chamber over-pressurization. Further assessment of this method will require that reaction chamber heat losses be reduced and that greater amounts of sodium chlorate be reacted per cycle. In addition to this, more research should be conducted concerning the reactivity and preparation of nanoscale cobalt oxide catalysts. Due to nanoparticle agglomeration, the specific surface area and consequently catalytic potential of the cobalt oxide was reduced. This increased the required reaction chamber temperatures and prevented this batch method from being viable from a power requirement standpoint. Future work is also needed to integrate a sodium chlorate oxygen generator into a fuel cell power system. One assumption during this project was that any power required to operate the oxygen system would be supplied by the fuel cell. Instead, similar literature systems assumed the use of heat exchangers coupled with exhaust gases from either high temperature solid oxide fuel cells or combustion power cycles, allowing them to meet their oxygen generation heat requirements.

Appendices

THIS PAGE INTENTIONALLY LEFT BLANK

Appendix A

Hydrogen and Oxygen Storage Selection

A.1 Reactant Storage Metrics

This approach is essential for comparing various combinations of oxygen and hydrogen storage systems and in making final design choices [9]. SE refers to specific energy density (kWh/kg), ED refers to volumetric energy density (kWh/L), O_2 and H_2 refer to the oxygen and hydrogen storage subsystems, H_2O refers to the product water storage subsystem and SS refers to the combined storage system. While the volume of the product water was accounted for, its weight was discounted due to conservation of mass. Additionally, the weight and volume of a product water storage tank were not considered:

$$SE_{H_2} = \frac{E_{SS}}{m_{H_2}};\ SE_{O_2} = \frac{E_{SS}}{m_{O_2}};\ SE_{H_2O} = \frac{E_{SS}}{m_{H_2O}}$$

$$ED_{H_2} = \frac{E_{SS}}{V_{H_2}};\ ED_{O_2} = \frac{E_{SS}}{V_{O_2}};\ ED_{H_2O} = \frac{E_{SS}}{V_{H_2O}}$$

$$SE_{SS} = \frac{E_{SS}}{m_{H_2} + m_{O_2}} = \frac{1}{\frac{m_{H_2}}{E_{SS}} + \frac{m_{O_2}}{E_{SS}}} = \frac{1}{\frac{1}{SE_{H_2}} + \frac{1}{SE_{O_2}}} = \boxed{\frac{SE_{H_2} SE_{O_2}}{SE_{H_2} + SE_{O_2}}} \quad \text{(A.1)}$$

$$ED_{SS} = \frac{E_{SS}}{V_{H_2} + V_{O_2} + V_{H_2O}} = \frac{1}{\frac{V_{H_2}}{E_{SS}} + \frac{V_{O_2}}{E_{SS}} + \frac{V_{H_2O}}{E_{SS}}} = \boxed{\frac{1}{\frac{1}{ED_{H_2}} + \frac{1}{ED_{O_2}} + \frac{1}{ED_{H_2O}}}} \quad \text{(A.2)}$$

Using 241.83 kJ/mol$_{H_2}$ for the LHV of hydrogen, taking the density of product water to be 1 kg/L and using the stoichiometric hydrogen and oxygen reaction for a fuel cell, the water term in the preceding equation can be reduced to 3.73 kWh/L:

$$SE_{H_2O} = \frac{241.83\,kJ}{1\,mol_{H_2}} \cdot \frac{1\,mol_{H_2}}{1\,mol_{H_2O}} \cdot \frac{1\,mol_{H_2O}}{0.018\,kg_{H_2O}} \cdot \frac{1\,hr}{3600\,sec} = 3.73\,\frac{kWh}{kg_{H_2O}}$$

$$ED_{H_2O} = 3.73\,\frac{kWh}{kg_{H_2O}} \cdot \frac{1\,kg_{H_2O}}{1\,L_{H_2O}} = \boxed{3.73\,\frac{kWh}{L_{H_2O}}} \quad \text{(A.3)}$$

Though not included in this thesis, Davies and Moore also showed that 3.73 kWh/L and 3.73 kWh/kg are the upper bounds for the volumetric and specific energy densities of underwater fuel cell power systems [9]. Assuming the previously used fuel cell efficiency of 60%, these values reduce to 2.24 kWh/L and 2.24 kWh/kg. These values are around five times greater than the energy densities of existing fuel cell power systems (see Figure 2-16) and indicate that there is still much room, at least theoretically, for these systems to improve.

A.2 Reactant Storage ED and SE Calculations

A.2.1 Hydrogen Storage

60% Lithium Hydride and 40% Light Mineral Oil Slurry

This hydrogen storage option, offered by Safe Hydrogen LLC, was advertised as having a gravimetric hydrogen density of 25.2% [34]. However, this is reduced to 6.4% after accounting for the weight of a stoichiometric amount of water needed to react with the hydride and the weight of the mineral oil. This is still a high gravimetric density for hydrogen storage systems, however it would be reduced further if the storage and operating equipment were considered.

$$LiH + H_2O = LiOH + H_2$$

$$1\ kg_{slurry} = 0.6\ kg_{LiH} + 0.4\ kg_{oil}$$

$$0.6\ kg_{LiH} \rightarrow 0.15\ kg_{H_2};\ \ 0.6\ kg_{LiH} \rightarrow 1.36\ kg_{H_2O}$$

$$Tot.\ Mix.\ Weight = 0.6\ kg_{LiH} + 0.4\ kg_{oil} + 1.36\ kg_{H_2O} = 2.36\ kg_{mix}$$

$$\rho_{mix,avg} = 0.92\ \frac{kg_{mix}}{L}$$

$$Wt.\%\ H_2 = \frac{0.15\ kg_{H_2}}{2.36\ kg_{mix}} = 0.064\ \frac{kg_{H_2}}{kg_{mix}} = 6.4\%$$

$$SE_{H_2} = \frac{241.83\ kJ}{1\ mol_{H_2}} \cdot \frac{1\ mol_{H_2}}{0.002\ kg_{H_2}} \cdot \frac{0.064\ kg_{H_2}}{1\ kg_{mix}} \cdot \frac{1\ hr}{3600\ sec} = \boxed{2.15\ \frac{kWh}{kg}}$$

$$ED_{H_2} = SE_{H_2} \cdot \rho_{mix,avg} = 2.15\ \frac{kWh}{kg_{mix}} \cdot 0.92\ \frac{kg_{mix}}{L} = \boxed{1.98\ \frac{kWh}{L}}$$

Aluminum

The analysis shown above was used to determine the energy densities of aluminum hydrogen storage. An average density of 1.27 kg/L was calculated for the aluminum and water mixture. We calculated a hydrogen gravimetric storage density of 3.7%, based on the mass of aluminum and a stoichiometric amount of water. This technology is still under development at MIT in conjunction with Lincoln Laboratory [35].

$$2Al + 6H_2O = 2Al(OH)_3 + 3H_2$$

$$SE_{H_2} = \boxed{1.24\ \frac{kWh}{kg}} \quad ED_{H_2} = \boxed{1.57\ \frac{kWh}{L}}$$

Compressed Hydrogen Gas at 5076 psi

Carbon composite hydrogen gas storage tank offered by Luxfer Cylinders [41].

$$M_{tank} = 138kg, M_{H_2} = 7.7kg, M_{tot} = 145.7kg, D = 0.415m, L = 3.128m, V_{tot} = 423.1L$$

$$E_{H_2} = 7.7\ kg_{H_2} \cdot \frac{1\ mol_{H_2}}{0.002\ kg_{H_2}} \cdot \frac{241.83\ kJ}{1\ mol_{H_2}} \cdot \frac{1\ hr}{3600\ sec} = 258.6\ kWh$$

$$SE_{H_2} = \frac{E_{H_2}}{M_{tot}} = \boxed{1.78\ \frac{kWh}{kg}} \quad ED_{H_2} = \frac{E_{H_2}}{V_{tot}} = \boxed{0.61\ \frac{kWh}{L}}$$

Cryogenic Liquid Hydrogen

Cryogenic stainless steel hydrogen storage tank used on the GM Hydrogen3 fuel cell vehicle [42].

$$M_{H_2} = 4.6\ kg,\ M_{tot} = 90\ kg,\ D = 0.4\ m,\ L = 1\ m,\ V_{tot} = 125.7\ L$$

$$E_{H_2} = 4.6\ kg_{H_2} \cdot \frac{1\ mol_{H_2}}{0.002\ kg_{H_2}} \cdot \frac{241.83\ kJ}{1\ mol_{H_2}} \cdot \frac{1\ hr}{3600\ sec} = 154.5\ kWh$$

$$SE_{H_2} = \frac{E_{H_2}}{M_{tot}} = \boxed{1.72\ \frac{kWh}{kg}} \quad ED_{H_2} = \frac{E_{H_2}}{V_{tot}} = \boxed{1.23\ \frac{kWh}{L}}$$

A.2.2 Oxygen Storage

CAN33 Oxygen Candle

Oxygen candle supplied by Molecular Products [43].

$$M_{O_2} = 4.64\,kg,\ M_{tot} = 12.74\,kg,\ D = 0.165\,m,\ L = 0.295\,m,\ V_{tot} = 6.32\,L$$

$$E_{O_2} = 4.64\,kg_{O_2} \cdot \frac{1\,mol_{O_2}}{0.032\,kg_{O_2}} \cdot \frac{1\,mol_{H_2}}{0.5\,mol_{O_2}} \cdot \frac{241.83\,kJ}{1\,mol_{H_2}} \cdot \frac{1\,hr}{3600\,sec} = 19.5\,kWh$$

$$SE_{O_2} = \frac{E_{O_2}}{M_{tot}} = \boxed{1.53\,\frac{kWh}{kg}} \quad ED_{O_2} = \frac{E_{O_2}}{V_{tot}} = \boxed{3.08\,\frac{kWh}{L}}$$

Compressed Oxygen Gas at 3000 psi

Carbon composite oxygen gas storage tank offered by Luxfer Cylinders [41].

$$M_{O_2} = 2.49\,kg,\ M_{tot} = 6.69\,kg,\ D = 0.173\,m,\ L = 0.529\,m,\ V_{tot} = 12.4\,L$$

$$E_{O_2} = 2.49\,kg_{O_2} \cdot \frac{1\,mol_{O_2}}{0.032\,kg_{O_2}} \cdot \frac{1\,mol_{H_2}}{0.5\,mol_{O_2}} \cdot \frac{241.83\,kJ}{1\,mol_{H_2}} \cdot \frac{1\,hr}{3600\,sec} = 10.44\,kWh$$

$$SE_{O_2} = \frac{E_{O_2}}{M_{tot}} = \boxed{1.56\,\frac{kWh}{kg}} \quad ED_{O_2} = \frac{E_{O_2}}{V_{tot}} = \boxed{0.84\,\frac{kWh}{L}}$$

Cryogenic Liquid Oxygen

Cryogenic liquid oxygen system offered by Sierra Lobo [14].

$$M_{O_2} = 50\,kg,\ M_{tot} = 63.6\,kg,\ D = 0.32\,m,\ L = 0.94\,m,\ V_{tot} = 75.6\,L$$

$$E_{O_2} = 50\,kg_{O_2} \cdot \frac{1\,mol_{O_2}}{0.032\,kg_{O_2}} \cdot \frac{1\,mol_{H_2}}{0.5\,mol_{O_2}} \cdot \frac{241.83\,kJ}{1\,mol_{H_2}} \cdot \frac{1\,hr}{3600\,sec} = 209.9\,kWh$$

$$SE_{O_2} = \frac{E_{O_2}}{M_{tot}} = \boxed{3.30\,\frac{kWh}{kg}} \quad ED_{O_2} = \frac{E_{O_2}}{V_{tot}} = \boxed{2.78\,\frac{kWh}{L}}$$

Ideal $NaClO_3$

$$NaClO_3 = NaCl + 1.5O_2$$

$$\rho_{NaClO_3} = 2.49\,\frac{kg}{L}$$

$$SE_{O_2} = \frac{241.83\,kJ}{1\,mol_{H_2}} \cdot \frac{1\,mol_{H_2}}{0.5\,mol_{O_2}} \cdot \frac{1.5\,mol_{O_2}}{1\,mol_{NaClO_3}} \cdot \frac{1\,mol_{NaClO_3}}{0.10644\,kg_{NaClO_3}} \cdot \frac{1\,hr}{3600\,sec} = \boxed{1.89\,\frac{kWh}{kg}}$$

$$ED_{O_2} = 1.89\,\frac{kWh}{kg} \cdot 2.49\,\frac{kg}{L} = \boxed{4.71\,\frac{kWh}{L}}$$

Ideal $LiClO_4$

$$LiClO_4 = LiCl + 2O_2$$

$$\rho_{LiClO_4} = 2.42\,\frac{kg}{L}$$

$$SE_{O_2} = \frac{241.83\,kJ}{1\,mol_{H_2}} \cdot \frac{1\,mol_{H_2}}{0.5\,mol_{O_2}} \cdot \frac{2\,mol_{O_2}}{1\,mol_{LiClO_4}} \cdot \frac{1\,mol_{LiClO_4}}{0.10639\,kg_{LiClO_4}} \cdot \frac{1\,hr}{3600\,sec} = \boxed{2.53\,\frac{kWh}{kg}}$$

$$ED_{O_2} = 2.53\,\frac{kWh}{kg} \cdot 2.42\,\frac{kg}{L} = \boxed{6.11\,\frac{kWh}{L}}$$

Appendix B

Oxidant and Catalyst Properties

Sodium Chlorate and Lithium Perchlorate:

Property	$NaClO_3$	$LiClO_4$
MW (g/mol)	106.44	106.39
ρ (kg/L)	2.49	2.42
$c_{p,s}$ (J/molK)	125.14	104.5
$c_{p,l}$ (J/molK)	258.75	161.2
h_{fus} (J/mol)	21830	29300
T_{melt} (°C)	248	236
n_{powder} (kmol/sec)	0.5206	0.3904

Catalysts for Thermal Decomposition:

Property	Co_3O_4	Co_2O_3	Cr_2O_3	MnO_2	Li_2O_2
MW (g/mol)	240.8	165.9	152.0	86.9	45.8
ρ (kg/L)	6.11	5.18	5.22	5.03	2.31
$c_{p,s}$ (J/molK)	123.4	123.4	118.7	54.1	89.7
$n_{catalyst}$ (kmol/sec)	7.12E-03	8.35E-02	6.83E-02	2.52E-02	1.23E-02

THIS PAGE INTENTIONALLY LEFT BLANK

Appendix C

Additional SEM Images

Unground, uncatalyzed sodium chlorate with gold nanoparticle sputter coating typical of SEM imaging:

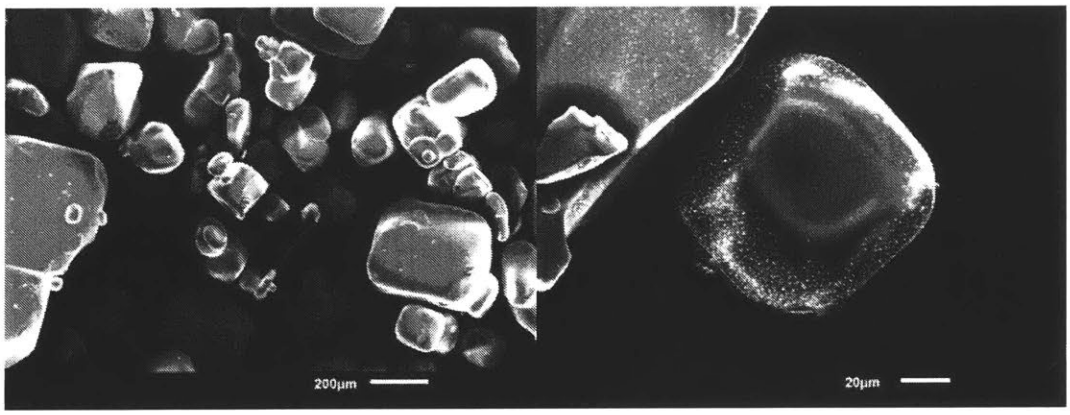

Unground sodium chlorate with microscale cobalt oxide catalyst:

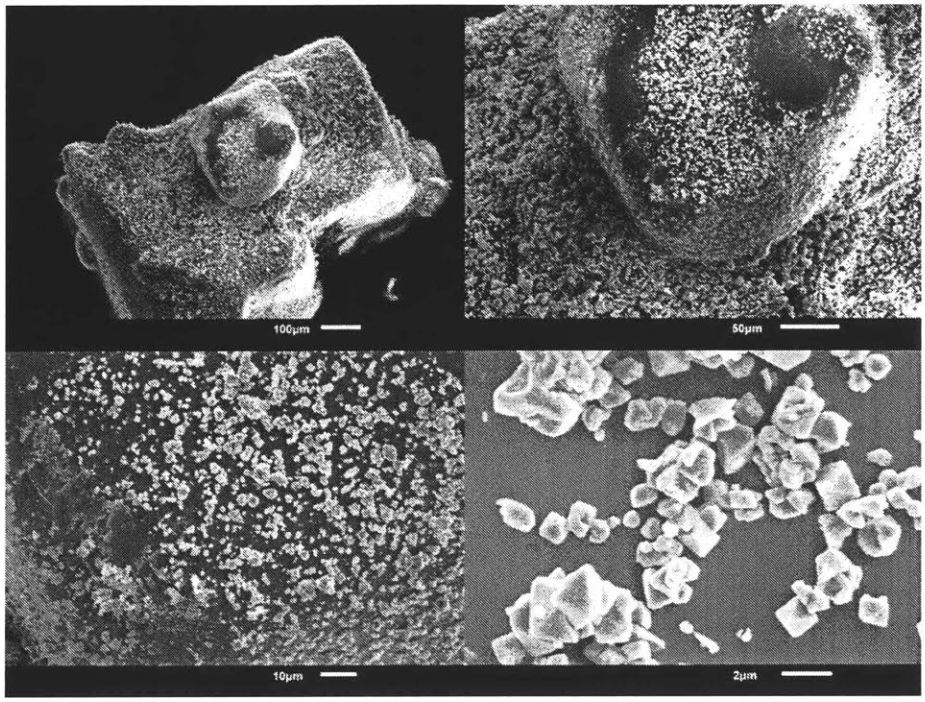

Twice ground sodium chlorate with nanoscale cobalt oxide:

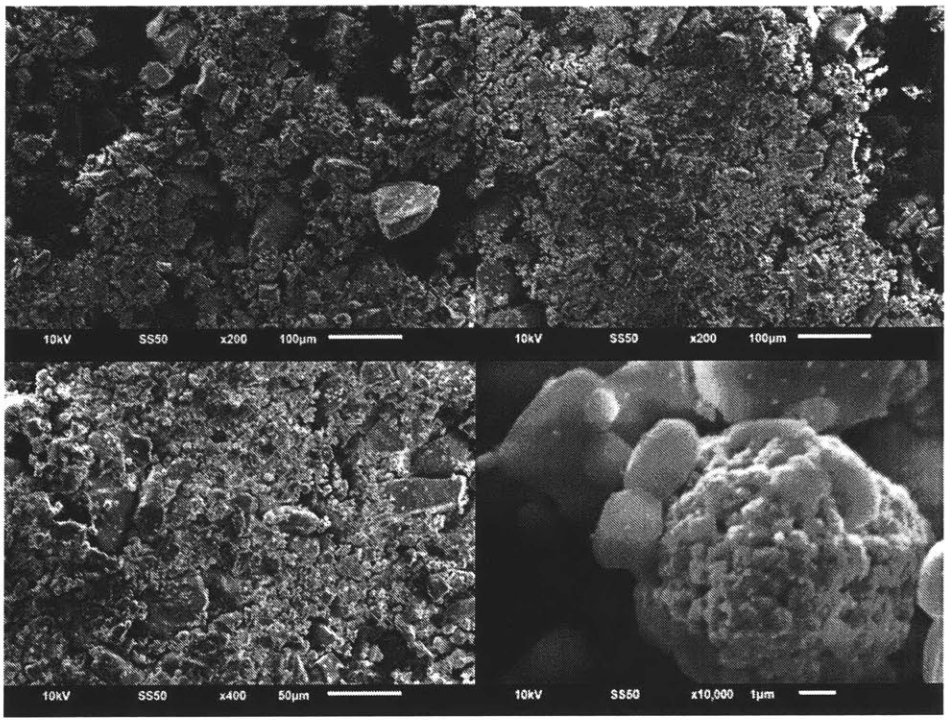

Bibliography

[1] Alan Burke. System modeling of an air-independent solid oxide fuel cell system for unmanned undersea vehicles. *Journal of Power Sources*, 2005.

[2] E. Shafirovich, A. Garcia, A.K. Narayana Swamy, D.J. Mast, and S.D. Hornung. On feasibility of decreasing metal fuel content in chemical oxygen generators. *Combustion and Flame*, 159(1):420–426, jan 2012.

[3] Edward Whitman. Air-independent propulsion (aip) technology creates a new undersea threat. *Undersea Warfare*, 2001.

[4] U212 and u214 submarines. URL `www.naval-technologies.com`.

[5] Hasvold. Transportation-submersibles: Batteries. *Encyclopedia of Electrochemical Power Sources*, pages 367–380, 2009.

[6] G Griffiths, J Jamieson, S Mitchell, and K Rutherford. Energy storage for long endurance auvs. pages 1–9, 2004.

[7] US Navy. The navy unmanned undersea vehicle (uuv) master plan. Technical report, 2004.

[8] Alejandro Mendez, Teresa Leo, and Miguel Herreros. Current state of technology of fuel cell power systems for autonomous underwater vehicles. *Energies*, 7(7): 4676–4693, jul 2014.

[9] Kevin Davies and Robert Moore. Uuv fceps technology assessment and design process. Technical report, Hawaii Natural Energy Institute, 2006.

[10] S. Ishibashi Hiroshi Yoshida, Toshiya Inada. Fuel cell system of auv urashima. 2004.

[11] G Reader. Power and oxygen sources for a diver propulsion vehicle. 2002.

[12] P Kallender-Umezu. Japan to make major switch on sub propulsion, Oct 2014. URL `www.pacom.mil`.

[13] K Swider-Lyons. Hydrogen fuel cells for unmanned undersea vehicle propulsion.

[14] Mark Haberbusch Bradley Stoops, Chinh Nguyen. Multifunctional cryogenic power system for unmanned underwater vehicles. 2009.

[15] Grant Thornton. A design tool for the evaluation of atmosphere independent propulsion in submarines. 1994.

[16] Hennessy P Jinks, J. *The Silent Deep: The Royal Navy Submarine Service Since 1945.* Penguin UK, Oct 2015.

[17] Meyer Markowitz. Lithium Perchlorate Oxygen Candle. *Industrial and Engineering Chemistry Research*, 3(4):321–330, 1964.

[18] Oxygen-generation systems. *Kirk-Othmer Encyclopedia of Chemical Technology*, pages 1–11, 2000.

[19] C Malich and T Wydeven. Catalyzed sodium chlorate candles, 1972.

[20] Junker S Willman C Peters J Martin J Pastula M Tang E Ghezel-Ayagh, H. Advances in design of solid oxide fuel cell hybrid power systems for underwater applications. *ECS Transactions*, pages 23–29, 2009.

[21] William (BNI) Batton, Kevin (BNI) Hotton, Jonathan (ARL) Peters, and Martin (ARL) Klanchar. Oxygen source for underwater vehicle fuel cells. Technical report, Office of Naval Research, 2002.

[22] Arthur Comey. *A Dictionary of Chemical Solubilities.* The Macmillan Company, 1921.

[23] Atherton Seidell. *Solubilities of Inorganic and Organic Compounds.* 1919.

[24] Andre Charette. Encyclopedia of reagents for organic synthesis.

[25] Meyers Scott Presley, Kenneth. Oxygen-generating liquid composition, 2015.

[26] Swartz Scott Presley, Kenneth. A new oxygen source for sofc based power systems for long duration uuvs. URL `fuelcellseminar.com`.

[27] Vickerman Adam Hart Douglas Crane, Jackson. A system for producing oxygen using sodium chlorate dissociation.

[28] Hart Douglas Rodriguez, Mario. Mechanically-actuated oxygen gas generation via sodium chlorate decomposition.

[29] M Burcat, A; Steinberg. The influence of some transition and inner transition metal oxides on the thermal decomposition of molten lithium perchlorate. *Journal of Inorganic and Nuclear Chemistry*, 30.

[30] James C Canon. Catalytic and Inhibiting Effects of Lithium Peroxide and Hydroxide on Sodium Chlorate Decomposition. *Industrial and Engineering Chemistry Research*, 34(9):3146–3148, 1995.

[31] T Wydeven. Catalytic decomposition of sodium chlorate. *Journal of Catalysis*, 19(2):162–171, nov 1970.

[32] Sigma aldrich product comparison guide, Feb 3, 2017. URL sigmaaldrich.com/catalog/substance.

[33] Thermo fisher scientific. URL alfa.com/en/catalog.

[34] Ronald Breault Andrew McClaine and Christopher Larsen. Hydrogen transmission/storage with metal hydride-organic slurry and advanced chemical hydride/hydrogen for pemfc vehicles, 2000.

[35] Johnny Slocum. The design of a power system using treated aluminum fuel. 2015.

[36] Chemical compatibility guide, 2013. URL habonim.com/pdg/engineering/corrosion_table.pdf.

[37] Apv corrosion handbook, 2008. URL spxflow.com/en/assets/pdf/apv_corrosion_handbook_1035_01_08_2008_US_tcm11-7079.pdf.

[38] Kevin Johnson Richard Hagar Alan McCarrick, Jon Haas. Us navy sodium chlorate oxygen candle safety. 2011.

[39] Allen Garcia. *On Feasibility of Reducing Metal Fuel Content and Operating Temperatures in Chemical Oxygen Generators.* PhD thesis, 2011.

[40] Heat tint (temper) colours on stainless steel surfaces heated in air, 2017. URL www.bssa.org.uk.

[41] Luxfer gas cylinders. URL www.luxfercylinders.com/products.

[42] Technical data of hydrogen3 liquid. URL archives.media.gm.com/about_gm/vehicle_tech/fuel_cell/vehicles/monaco/hydrogen/technical_liquid.htm.

[43] Chemical oxygen generation. URL www.molecularproducts.com.